The Role of BASP1 in Neural Development

by

Kaitlin A. Mac Donald

Submitted in partial fulfilment of the requirements
for the degree of Master of Science

at

Dalhousie University
Halifax, Nova Scotia
November 2019

Table of Contents

List of Tables

List of Figures

Abstract

BASP1 (brain acid soluble protein 1) is highly expressed in the nervous system throughout development. While its roles at the neuromuscular junction and in certain non-neuronal tissues have been previously characterized, its function in the neural tube is still unclear. Using the chicken (*Gallus gallus*) as a model, I show that *BASP1* is expressed in the neural tube exclusively in differentiated neurons, in contrast with previous expression data. Using gain- and loss- of function approaches, BASP1 overexpression was shown to cause the ectopic placement of neural progenitor cells. These ectopic cells were found in the neural tube marginal zone, normally the site of only differentiated neurons. This indicates a possible role for BASP1 in eliminating apical cell polarity in progenitor cells, in opposition to the role of the protein MARCKS. I also demonstrated that BASP1 knockdown by dsRNA-mediated interference led to a transient decrease in axonal complexity of hindbrain neurons.

List of Abbreviations Used

%GC: percent of DNA composed of guanine and cytosine

Bak: BCL2 antagonist/killer

BASP1: brain acid soluble protein 1

BIRP: BASP1 immunologically related protein

BNEMF: BASP N-end myristoylated fragments

BTX: botulinum toxin A

CAP23: 23 kDa cortical cytoskeleton-associated protein; also known as BASP1

cBASP1: chicken BASP1

CMV-IE promotor: cytomegalovirus-immediate early promotor

DAPI: 4′,6-diamidino-2-phenylindole

DEPC: diethyl pyrocarbonate

DIG: digoxigenin

DRG: dorsal root ganglia

dsRNA: double-stranded RNA

DTT: dithiothreitol

EDTA: ethylenediaminetetraacetic acid

GAP43: growth-associated protein 43

GFP: green fluorescent protein

HH stages: Hamburger-Hamilton stages

hpe: hours post-electroporation

IF: immunofluorescence

IRES: internal ribosome entry site

ISH: *in situ* hybridization

IZ: intermediate zone

MARKS: myristoylated alanine-rich protein C-kinase substrate

MZ: marginal zone

NAP22: 22 kDa neuronal tissue-enriched acidic protein; also known as BASP1

NBT/BCIP: nitro blue tetrazolium / 5-bromo-4-chloro-3-indolyl phosphate

NCAM: neural cell adhesion molecule

OCT compound: optimal cutting temperature compound

PBS: phosphate-buffered saline

PBT: PBS–Triton-X100 (0.05% Triton-X100 unless otherwise noted)

PEST sequence: region of peptide rich in proline (P), glutamic acid (E), serine (S), and threonine (T)

pHH3: phosphohistone H3 (Ser10)

PIP−2: phosphatidylinositol 4,5-bisphosphate

PIP3: phosphatidylinositol (3,4,5)-trisphosphate

PML bodies: promyelocytic leukemia protein bodies

RISC: RNA-induced silencing complex

RNAi: RNA interference

rNTP: ribonucleoside triphosphate

SDS-PAGE: sodium dodecyl sulfate–polyacrylamide gel electrophoresis

siRNA: small interfering RNA

SNAREs: SNAP receptor proteins

SSC: saline sodium citrate

ssRNA: single-stranded RNA

TBS: Tris-buffered saline

TRITC: tetramethylrhodamine

VAMP2: vesicle-associated membrane protein 2

VZ: ventricular zone

WT1: Wilms' tumor suppressor protein 1

Acknowledgments

Thanks first and foremost must go to Dr. Angelo Iulianella, my thesis supervisor. He provided excellent guidance throughout the research process, assisted with the imaging, and was always sincerely invested in my success. As well, his editing was immensely useful, and this thesis would be half the document it is without it. Thanks as well go to my fellow graduate students, Danielle and Sam, and our research assistant Karolynn. All three taught me much of the technical skills necessary for my research and provided effective technical help. Thanks to my thesis committee, Dr. Kazue Semba and Dr. William Baldridge, and my external examiner, Dr. Boris Kablar, for their critiques and corrections. And my deepest gratitude to my mom and dad, my siblings Aislin and Devin, and my friend Andrew. Before and throughout this degree they all showed me so much how much they cared about me, believed in me unwaveringly, and gave me so much encouragement. Special thanks to Mom and Ash, for exemplifying the hard work and determination it takes to get a Masters degree. And thanks to Andrew for listening to many, many hours of impassioned and enthusiastic and deeply technical explanations of "small things that nobody cares about".

Chapter 1: Introduction

Apicobasal organization of the neural tube

During neural development, the neural tube progresses from undifferentiated neural progenitor cells to a central nervous system composed of many highly specialized cell types. Maturation of the neural tube is mostly from progenitor cell proliferation and differentiation, with little apoptosis or respecification (Kicheva et al., 2014). Consequently, the spatial organization of these progenitor cells is important. The movement of progenitors and their descendants along the apicobasal axis of the neural tube is critical for both tissue organization and for exposure to the correct pro- or anti-differentiation signals.

Progenitor cells reside along the apical side of the neural tube, forming the ventricular zone. On the most apical side of the ventricular zone are neuroepithelial cells and radial glia (Laguesse et al., 2015). These apical progenitors form pseudostratified epithelium: there are different "layers" of progenitor somata, but each cell is connected to both the apical and basal side of the neural tube via long cell processes (Miyata, 2008). In the basal ventricular zone and even more basal subventricular zone are the intermediate progenitors and outer radial glia (Laguesse et al., 2015). Intermediate progenitors have a more limited differentiation potential than apical progenitors (Noctor et al., 2004). Both intermediate progenitors and outer radial glia are not attached to the apical surface during mitosis, and possibly elsewise too (Noctor et al., 2008; Fietz et al., 2010). Apical progenitor cells usually either divide symmetrically to make more progenitors or divide asymmetrically to make a progenitor cell and a cell that will differentiate or an intermediate progenitor (Noctor et al., 2008). Which type of division occurs is based on the presence of signals that inhibit or promote differentiation; the ever-changing balance of these signals is what drives neural development (Laguesse et al., 2015). These signals are possibly received via the apical and/or basal processes present in apical progenitors but not intermediate progenitors (Noctor et al., 2008). Additional rounds of progenitor division not leading to differentiation (and thus creating more cells in total) is thought to be involved in the evolution of cerebral cortex complexity in mammals (Martínez-Cerdeño et al., 2006). Progenitor daughter cells that differentiate into neurons lose their

apical polarity and become post-mitotic (Das and Storey, 2014; Frade and Ovejero-Benito, 2015). In the future spinal cord, cells move outwards as they differentiate. Basally to the ventricular zone, the intermediate zone (or mantle layer) contains some progenitors and the soma of differentiated neurons; this zone is the future spinal cord grey matter. The outgrowth of axons forms the marginal zone around the periphery of the basal neural tube; this will later become the white matter of the spinal cord (Kaufman and Bard, 1999). In the dorsal root ganglia (DRG) along the future spinal cord, neural crest cells form sensory neurons (Chen et al., 2017).

It is not just the neural tube as a whole that is polarized: neuroepithelial cells and radial glia also have apicobasal polarity. At this stage of development, the apical surface of the neural tube consists of the apical cell membrane of the progenitors along the neural tube lumen, while the basal surface is the pial basement membrane (Halfter et al., 2002; Saker et al., 2016). Both apical progenitor types are attached to both sides of the neural tube by long processes (Rakic, 2003; Laguesse et al., 2015). In radial glia, the basal process is inherited by only one daughter cell, with the other daughter usually differentiating (Alexandre et al., 2010). On their apical membrane neuroepithelial cells and radial glia have a primary cilium. This cilium projects from a basal body–forming centrosome into the cerebrospinal fluid of the neural tube lumen. There, it detects signals that keep the cell in a proliferative state, including Sonic Hedgehog and WNT (Louvi and Grove, 2011). The primary cilium is only present during interphase, as its centrosome is used in the mitotic spindle apparatus (Seeley and Nachury, 2010). During G2 of the cell cycle, the primary cilium shortens, and at the beginning of mitosis both the membrane and basal body are internalized. Only one daughter cell will inherit the centrosome with the attached ciliary remnant, and this cell can quickly regrow the primary cilium. The other daughter cell either slowly grows a new primary cilium from scratch, or differentiates (Paridaen et al., 2013). Differentiated cells detach from the apical surface via apical abscission, a shedding of the apical-most cell membrane. Newly differentiated cells, as marked by the expression of NEUROM, undergo a constriction of a subapical cable of actin. The primary cilium stays attached to the abscised apical membrane while its centrosome stays with the cell. Apical abscission is necessary for the expression of p27/Kip1, which causes exit from the cell cycle (Das and Storey, 2014). Apicobasal

polarity, as manifested by the cell processes and the primary cilium, is critical for maintaining the balance of proliferation versus differentiation.

Neuroepithelial cells and radial glia undergo interkinetic nuclear migration: the soma (and nucleus too in neuroepithelial cells) migrates between the apical and basal ventricular zone through the cell cycle (Miyata, 2008; Laguesse et al., 2015). Progenitors start at the apical surface and move basally during G1. They are at the basal surface during S phase. During G2, cells move apically to then again be at the apical surface for mitosis (Miyata, 2008). Movement apically requires both microtubules and microtubule-associated proteins such as motors (Tsai et al., 2010). It is unclear if actin filaments also have a role; however, they do seem to be involved in the apical rounding of the cell prior to mitosis (Spear and Erickson, 2012). It is also unclear how basal migration is achieved – like apical movement, it may involve microtubules and/or actin filaments, or could be a passive process (Laguesse et al., 2015). By spreading out soma along the tissue, interkinetic nuclear migration allows more cells to fit into one layer of epithelium (Miyata, 2008). As well, interkinetic nuclear migration may control exposure to pro- or anti-differentiation signals. For example, basally-located nuclei may be exposed to less Delta-Notch signaling, and thus differentiate (Bene et al., 2008). A visualization of interkinetic nuclear migration and of neural tube apicobasal polarity can be seen in **Figure 1**.

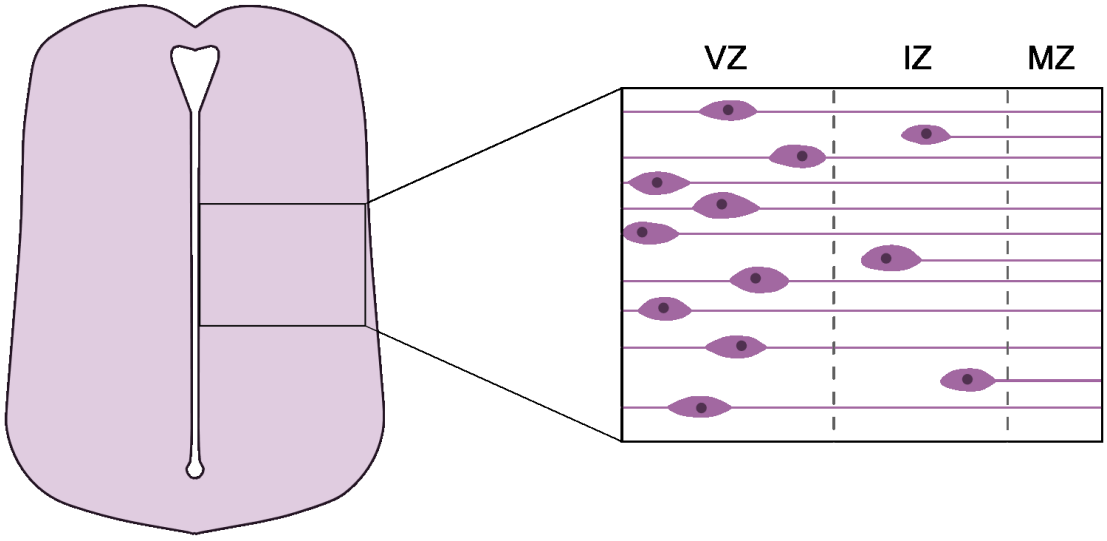

Figure 1. Apicobasal polarity in the neural tube. The newly differentiating neural tube (around chick E4.5) is split into three layers. In the ventricular zone, progenitor cells form a pseudostratified epithelium, with cells moving through the layer during the cell cycle. Differentiated cells lose their connection to the apical side of the neural tube and move basally into the intermediate zone. From there, neurons grow axons out into the marginal zone, from where axons grow to their eventual target. VZ = ventricular zone, IZ = intermediate zone, MZ = marginal zone.

The cytoskeleton

As spatial organization is important for exposure to pro- or anti-differentiation signals, the cytoskeleton plays a critical role in neural development. The cytoskeleton is involved in a number of structural cell functions, including but not limited to cell shape and polarity, withstanding mechanical stress, cell movement, the transport and subcellular location of vesicles, organelles, and mRNA, the mitotic spindle apparatus, and cytokinesis (Alberts et al., 2007).

Three different types of protein filaments make the cytoskeleton. First are microtubules, hollow cylinders composed of repeated dimers of α- and β-tubulin (Bryan and Wilson, 1971). Microtubules are mainly involved in organelle positioning and vesicle transport, and are part of the spindle apparatus during mitosis (Wade and Hyman, 1997). In animal cells, the interphase location of microtubules differs: in proliferating cells, microtubules are anchored at the centrosome and radiate outwards; in differentiated cells, neither is the case (Bartolini and Gundersen, 2006). Microtubules are also present in cilia and flagella (Wade and Hyman, 1997). The second major cytoskeleton component are actin filaments, also known as microfilaments or F-actin. Actin filaments are 2-stranded helical polymers of actin monomers (G-actin), and are responsible for cell shape and movement (Hanson and Lowy, 1963; Pollard and Cooper, 2009). They are found in several locations in the cell, primarily underlying the cell membrane and in cell projections such as lamellipodia and filopodia (Michelot and Drubin, 2011). In cytokinesis, actin filaments are part of the contractile ring that separates cells (Sanger, 1975). The final part of the cytoskeleton is intermediate filaments. This is a heterogenous group of different fibrous subunits. Classes I and II include keratins; III includes vimentin, glial fibrillary acidic protein, desmin and peripherin; IV includes neurofilament proteins and nestin; and V includes lamins. As may be expected from this diversity, intermediate filaments provide mechanical strength in a wide variety of contexts, including hair, axons, and the nuclear lamina (Oshima, 2007). Some cells, such as oligodendrocytes, contain no intermediate filaments (Richter-Landsberg, 2008).

The cytoskeleton is dynamic, constantly forming and breaking down in response to the needs of the cell (Janmey, 1998). Microtubules and actin filaments in particular are polarized, with the plus end assembling and disassembling faster than the opposite minus

end (Stossel, 1989; Howard and Hyman, 2003). Cytoskeletal distribution and dynamics are regulated by associated proteins that transduce information from various signaling pathways. These proteins include but are not limited to microtubule-associated proteins (including tau) for microtubules (Drechsel et al., 1992), and spectrin, formin, and CapZ for actin filaments (Liu et al., 1987; Caldwell et al., 1989; Pruyne et al., 2002). Also associated with the cytoskeleton are motor proteins, which move along the cytoskeleton and may carry cargo such as vesicles and organelles. The motor domain of these proteins hydrolyses ATP, causing a conformational change, which in turn causes binding and unbinding to the filament in question (Finer et al., 1994; Hirokawa, 1998). For microtubules, kinesins mostly move to the plus end and dyneins move to the minus end (Hirokawa, 1998), while myosins mostly move to the plus end of actin filaments (Finer et al., 1994; Wells et al., 1999).

The cytoskeleton in neurite outgrowth

Neurons are in part characterized by their long cell projections – dendrites and axons – that connect them to other cells and tissues. In the neural tube, the outgrowth of these neurites occurs after commitment to a neuronal fate, growing from the soma to wherever it is destined to innervate (Geraldo and Gordon-Weeks, 2009; Compagnucci et al., 2016). Neurites grow in response to attraction and repulsion cues found on the extracellular matrix, on cell membranes, and as long-range concentration gradients (Chilton, 2006). At the tip of each neurite is the growth cone, which transduces guidance cues into changes in the cytoskeleton (Chilton, 2006; Cammarata et al., 2016). During neurite outgrowth, the growth cone may respond to several signals sequentially; that is, reach a certain point then shift directions. Turning too requires reorganization of the cytoskeleton. The exact mechanism of this coordination is unclear but involves plus-end tracking proteins, which add or remove tubulin to the plus end of microtubules and interact with actin filaments (Cammarata et al., 2016). Consequently, microtubules and actin filament dynamics must coordinate to elongate the neurite and steer the growth cone (Geraldo and Gordon-Weeks, 2009).

Different domains of the growth cone have varying cytoskeletal composition and organization. More distally, the growth cone is spread out and there are more actin

filaments; more proximally, it narrows and microtubules dominate (Geraldo and Gordon-Weeks, 2009). As the growth cone advances, distal domains shift to a proximal identity (Geraldo and Gordon-Weeks, 2009). The most distal is the peripheral domain of filopodia and lamellipodia. Both contain actin filaments: in filopodia as parallel bundles while in the lamellipodia as a branched network. As well, filopodia actin filament bundles are often associated with unbundled microtubules (Lewis and Bridgman, 1992; Schaefer et al., 2002). Filopodia are the site of guidance cue signal transduction in the growth cone, and the extension and retraction of filopodia and lamellipodia are what cause form outgrowth (Gupton and Gertler, 2007; Geraldo and Gordon-Weeks, 2009). Filopodia extend when actin monomers are added to actin filaments at the tip, while filopodia retraction occurs when actin filaments translocate away from the tip (retrograde flow) (Okabe and Hirokawa, 1991). Next to the peripheral domain is the transition zone. Like the former, it contains bundles of actin filaments and unbundled microtubules. It is also where actin arcs form, antiparallel bundles of actin and myosin II (Schaefer et al., 2002; Medeiros et al., 2006). In the central domain, these actin arcs start to compress microtubules together. The central domain also contains vesicles and mitochondria (Burnette et al., 2008; Geraldo and Gordon-Weeks, 2009). In the wrist of the growth cone, microtubules become fully compressed into bundles (Burnette et al., 2008). This organization continues into the shaft of the neurite (Conde and Cáceres, 2009).

Of neurites, most become dendrites while one, associated with the centrosome, differentiates into the axon (Calderón de Anda et al., 2005). Dendrites and axons have similar cytoskeletal compositions. As mentioned above, in neurites microtubules are bundled. Different microtubule-associated proteins dominate in different neurites: MAP2 is mostly found in dendrites while tau is mostly found in axons (Conde and Cáceres, 2009). Microtubule polarity also differs. In axons, all microtubules are oriented in the same direction, with the minus end oriented towards the soma. In dendrites, orientation varies – near the growth cone, microtubules have the same polarity as in the axon, while in the middle of the dendritic shaft, about half have their plus end distal and half proximal (Baas et al., 1988). In axons, microtubules are the main structural component, with neurofilaments providing additional support (Alberts et al., 2007; Arnold and Gallo, 2014). Structural support is especially important for axons, owing to their potentially

great length – in humans, axons can be up to a meter long (Alberts et al., 2007). In vertebrates, axonal elongation is associated with an increase in microtubule length and number, followed by an even greater increase in length but a decrease in number (Miller and Suter, 2018). Microtubule stability differs along the axon. More proximally, α-tubulin is acetylated, making the microtubule more stable. More distally (and in short unbranched neurites), α-tubulin is tyrosinated, making the microtubule more dynamic (Conde and Cáceres, 2009). Microtubules are also the scaffold for axonal transport, with kinesins responsible for anterograde transport and dyneins for retrograde transport (Hirokawa, 1998). Proteins are mostly translated in the soma and must be transported along the axon. However, some mRNA is translated at the distal end of the axon and must be transported as well (Compagnucci et al., 2016). In particular, while most actin is synthesized outside of the axon, β-actin mRNA is also in the axon and is translated in response to particular extracellular signals (Black and Lasek, 1979; Willis et al., 2007). In dendrites, actin is present as long filaments under the cell membrane and mostly along the shaft of the dendrite (Xu et al., 2013). In axons, actin filaments have more complex arrangements: waves, rings, trails, and patches. These have mostly only recently been studied, especially in the context of neurons: waves have been known for about 2 decades but were dismissed as an artifact, while rings and trails have only been discovered within the past decade (Roy, 2016). Actin waves consist of actin filaments fanned out at acute angles to the length of the axon, flaring out the cell membrane. They appear periodically and move slowly along the axon from base to tip (Katsuno et al., 2015). Microtubules have a still unclear function in actin waves, as waves are disrupted with application of the microtubule-depolarizing agent nocodazole (Ruthel and Banker, 1998). Actin waves also had a high concentration of GAP43 (Ruthel and Banker, 1998), a protein which will be discussed further below. Actin waves seem to have some role in axon elongation, but have also been seen in multiple non-neural cell types (Katsuno et al., 2015; Roy, 2016). A second type of structure, actin rings, consist of periodic actin filament lattices circumscribing the axon under the cell membrane (Xu et al., 2013). These rings alternate along the axon with spectrin tetrameters that seem to act as spacers (Xu et al., 2013). Together, they may provide mechanical support (Xu et al., 2013). Yet another type of actin structure are actin trails, which are regularly spaced spots of continuous actin

filament assembly and disassembly. They require formin for their elongation, but not nucleation (Ganguly et al., 2015). Elongation can be either anterograde or retrograde, with the former more common (Ganguly et al., 2015). Unlike with actin waves, microtubules do not seem to have a role in actin trails (Ganguly et al., 2015). The function of actin trails is still unknown (Roy, 2016). Finally, actin patches are actin filament meshes similar to those in the growth cone lamellipodia (Watanabe et al., 2012). Patches are present in the axon initial segment, where they may be part of the filter that prevents non-axonal cargo from entering (Watanabe et al., 2012). As well, actin patches are also found more distally, where they are precursors to filopodia formation; this in turn leads to the formation of collateral branches (Spillane et al., 2011). They localize with phosphatidylinositol (3,4,5)-triphosphate (PIP_3) microdomains on the cell membrane (Ketschek and Gallo, 2010). In the axon shaft, actin patches exist only briefly – less than a minute (Spillane et al., 2011). Patches are also present in dendrites, where they too lead to filopodia formation (Korobova and Svitkina, 2009). The presence and concentration of the various actin filament structures changes through development, as seen by those that have been studied in the development of cultured hippocampal neurons. In these cultures, actin waves appear in stage 2 neurons (prior to axogenesis; about 1 day *in vitro*), and are more concentrated in the future axon (Flynn et al., 2009). Waves eventually diminish in number (Roy, 2016). Actin rings appear in the axon in stage 3 neurons (axonal outgrowth; around 2 days *in vitro*), and slowly spread along the entire axon (Zhong et al., 2014). Actin trails have been seen in stage 5 neurons (axon initial segment, spines, and synapses forming; 7 to 10 days *in vitro*), but have not been studied earlier in development (Roy, 2016). Actin patches too do not seem to have been studied earlier, but are present from at least 10 days *in vitro* onwards in dendritic spines (Korobova and Svitkina, 2009).

BASP1

Brain acid soluble protein 1 (BASP1; previously NAP22 or CAP23) is a protein expressed in the nervous system, kidney, testes, spleen, and thymus (Mosevitsky et al., 1997). Its intracellular location is tissue specific. In the nervous system, BASP1 is found in a granular pattern under the cell membrane, while in the kidneys, BASP1 is in the nucleus (Widmer and Caroni, 1990; Carpenter et al., 2004). In the chicken (*Gallus*

gallus), the *BASP1* gene has two exons, with the protein-coding region solely in the second. This produces a transcript of 980 base pairs, translating to 244 amino acids (Zerbino et al., 2018). The initiator methionine is removed, bringing the final count to 243 residues (UniProt Consortium, 2019a). BASP1 is highly hydrophilic with basic N- and C-termini flanking acidic and proline-rich regions (Widmer and Caroni, 1990). BASP1 contains several PEST sequences (areas rich in Pro, Glu, Ser, and Thr), which are characteristic of proteins with high turnover; the number of PEST sequences per BASP1 varies with species (Mosevitsky et al., 1997). BASP1 is fairly well conserved between species, as shown in **Table 1** and **Figure 2**. Chicken, human, mouse, rat, and zebrafish BASP1 are about 21.5% identical, and the first four excluding zebrafish are about 43.5% identical. Antibodies against BASP1 however tend to be species-specific (Mosevitsky et al., 1997).

Table 1. Similarity of BASP1 among vertebrates.

Species	Ascension number	Number of amino acids	Similarity
Chicken (*Gallus gallus)*	P23614	244	
Human (*Homo sapiens*)	P80723	227	21.484%
Mouse (*Mus musculus*)	Q91XV3	226	
Rat (*Rattus norvegicus*)	Q05175	220	43.496%
Zebrafish (*Danio rerio*)	Q1RM09	197	

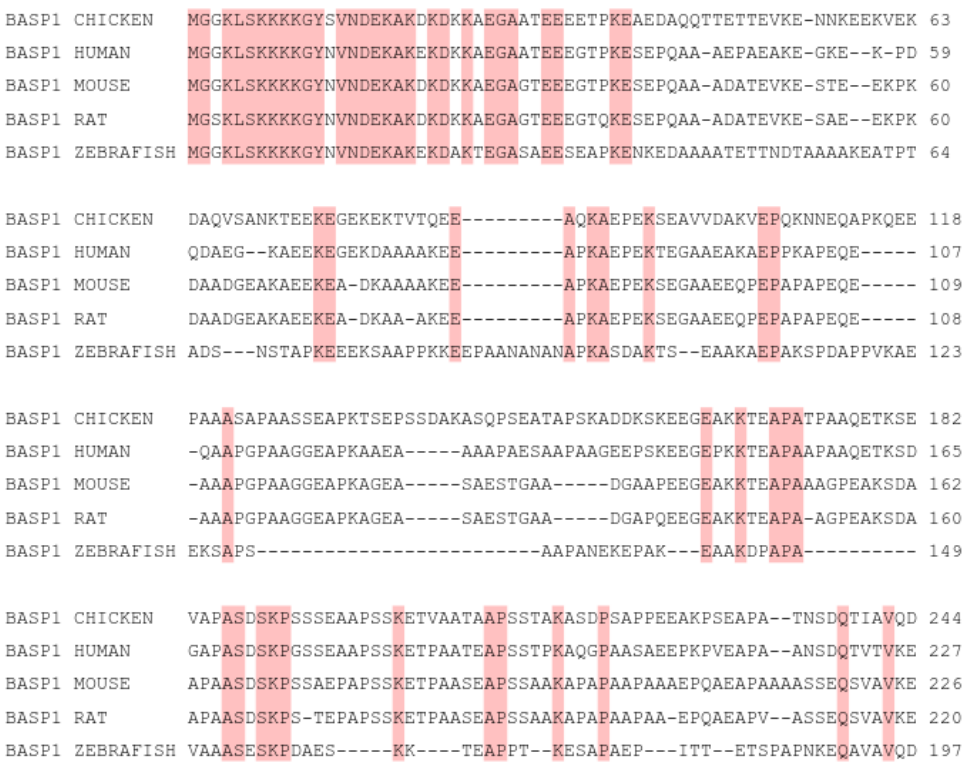

Figure 2. BASP1 amino acid alignment among vertebrates. Red indicates where the sequences are identical. For sequence ascension numbers, see **Table 1**.

BIRPs (BASP1 immunologically related proteins) or BNEMFs (BASP N-end myristoylated fragments) are abbreviated BASP1 sequences that are missing amino acids from their C-terminal end. They are found in mammals and chicken and can comprise 50 to 60% of total BASP1 in a given tissue. These fragments are not the result of splicing (as *BASP1* has only 1 protein-coding exon), and are possibly the result of premature synthesis cessation, mRNA editing, and/or proteolysis (Zakharov et al., 2003; Kropotova et al., 2013). There are at least 6 different lengths of fragments, which appear and accumulate at different times and durations during development; in the rat they first appear at E13 to 15 (Kropotova et al., 2013). Fragments share at least one of the full protein's post-translational modifications (Zakharov et al., 2003).

BASP1 is subject to several post-translational modifications (**Figure 3**). Most notably, it has a myristoyl group attached to Gly1 at the N-terminus, creating a hydrophobic region (Takasaki et al., 1999). This hydrophobicity, along with electrostatic interactions with several lysines near the N-terminus, allows BASP1 to attach to the cell membrane. *In vivo*, most BASP1 appears to be myristoylated (Mosevitsky et al., 1997). BASP1 is also phosphorylated at Ser6 by protein kinase C (Maekawa et al., 1994). The rate of phosphorylation increases with BASP1 myristoylation but is also hampered by the electrostatic interactions of BASP1's N-terminal lysines with the cell membrane. Phosphorylation thus weakens BASP1's attachment to the membrane (Mosevitsky et al., 1997; Takasaki et al., 1999). BASP1 can also bind strongly to calmodulin in a calcium-dependent manner (Maekawa et al., 1994). BASP1 has no canonical calmodulin-binding site. Instead, calmodulin binds to the myristoyl group with the hydrophobic pockets of calmodulin interacting with the acyl chain, instead of what would usually be hydrophobic amino acids on the target protein. Lys6, 7, 8, and 9 on BASP1 are important for calmodulin binding: there is almost complete binding with just the first 9 residues of BASP1, less with the first 6 and 7 residues, and none with just the first 3 (Takasaki et al., 1999). Calmodulin binding is inhibited by phosphorylation at Ser6 by protein kinase C (Maekawa et al., 1994). The post-translational modifications of BASP1 are important for its localization, and thus, its function.

Figure 3. Sites of post-translational modifications and notable amino acid sequences in chicken BASP1. M = myristoylation site, P = phosphorylation site, CaM = calmodulin binding site, NLS = nuclear localization sequence, PEST = PEST sequence.

BASP1 is similar in structure and function to the proteins GAP43 (growth-associated protein 43; also known as neuromodulin) and MARCKS (myristoylated alanine-rich protein C-kinase substrate). GAP43 and MARCKS have analogous but not homologous protein sequences to BASP1: all have PEST sequences and are high in Pro, Ala, Ser, Lys, and Glu (Mosevitsky et al., 1997; Wiederkehr et al., 1997). BASP1, GAP43, and MARCKS can be expressed simultaneously in the same neuron. All are found in potentially overlapping clusters along the cell membrane and are associated with the cytoskeleton. They also have similar post-translational modifications. Firstly, all are acylated – GAP43 with palmitic acid and BASP1 and MARCKS with myristic acid. Secondly, they have the same mutually exclusive protein kinase C phosphorylation versus calmodulin binding, although BASP1 has less phosphorylation and stronger calmodulin binding than GAP43 (Maekawa et al., 1994; Wiederkehr et al., 1997). Overexpression of all 3 proteins induces the formation of blebs and filopodia (Wiederkehr et al., 1997). Consequently, these three proteins can partially substitute for each other *in vivo*. At the neuromuscular junction, the sprouting defects seen in BASP1 knockout mice were not present when GAP43 was knocked in (Frey et al., 2000). However, in DRG neurons, knocking in GAP43 only restored cell morphology in BASP1 knockouts if that particular cell did not already have high endogenous levels of GAP43 (Frey et al., 2000). It is possible that GAP43 and MARCKS have identical or similar functions as BASP1, but in response to different signals (Caroni et al., 1997). For example, GAP43 potentiates NCAM-mediated neurite outgrowth, while BASP1 potentiation is independent of NCAM (Korshunova et al., 2008). It is as of yet unclear the purpose or cause of having three such partially redundant proteins.

Like GAP43 and MARCKS, BASP1 can be found in a granular pattern along the inner leaflet of the cell membrane (Widmer and Caroni, 1990). Specific lipid components of the cell membrane are not evenly distributed around the cell. Cholesterol and glycosphingolipids are particularly concentrated in lipid rafts, also known as membrane microdomains. Lipid rafts are thought to be involved in signaling, as many signaling pathway proteins partition to lipid rafts (Pike, 2003). BASP1 (and GAP43) fractionate with lipid rafts in tissue from 2-week-old rats and bind to liposomes in a cholesterol-dependent manner. This binding is inhibited by calmodulin and requires the presence of

acid phospholipids (Maekawa et al., 1999; Laux et al., 2000). One such phospholipid is phosphatidylinositol 4,5-bisphosphate (PIP_2): at lipid rafts, PIP_2 can localize signaling pathway components. PIP_2 is an important second messenger for many G protein–coupled receptors, where it is hydrolyzed by phospholipase C to inositol triphosphate and diacylglycerol. As well, PIP_2 binds to regulators of actin filaments, and connects the actin cytoskeleton to the cell membrane (Czech, 2000). Like BASP1, PIP_2 can also be found in clusters along the membrane. BASP1, GAP43, and MARCKS clusters all colocalize with clusters of PIP_2, and PIP_2 is accumulated at lipid rafts by binding to the effector domains of BASP1, GAP43, and MARCKS (Laux et al., 2000). Consequently, BASP1, GAP43, and MARCKS may function by interacting with other lipid raft components that too localize with PIP_2.

Like PIP_2, BASP1 is involved in the regulation of the actin cytoskeleton. In DRG sensory neuron cell cultures, similar morphologies are seen with both *BASP1* knockout and with actin polymerization inhibition (Frey et al., 2000). As well, in PC12 cells, BASP1 overexpression potentiates acquisition of actin-based filopodia and spikes. This is accompanied by less actin (as stained by phalloidin) outside the periphery of the cell. BASP1 overexpression also potentiates nerve spreading and outgrowth, and this is negated when cells are treated with the PIP_2 sequestering agent neomycin: cells become radially symmetrical, and filopodia and lamellae evenly distributed. A possible chain of events is that BASP1 modulates PIP_2, which modulates actin regulating proteins, which modulate actin (Laux et al., 2000). BASP1 also binds to the α subunit of CapZ, a plus end actin filament capping protein that promotes actin polymerization; however, BASP1 does not alter CapZ's effect on actin nucleation. It is possible that this interaction could be involved in anchoring actin to the cell membrane, although BASP1 myristoylation is not required for its binding to CapZ (Odagaki et al., 2009). Based on its induction of changes in cell morphology, its interaction with PIP_2, and its binding to CapZ, BASP1 seems to be involved in the localization or accumulation of actin filaments at the cell membrane.

In addition to its functions at the cell membrane, BASP1 can also act in the nucleus as a transcriptional corepressor. WT1 is a transcriptional regulator that targets genes for growth factors and regulators of cell division, and is named for its aberrant expression in the nephropathic Wilms' tumor (Carpenter et al., 2004). While WT1 can act

as a transcriptional activator, its N terminal region can suppress this activity (Carpenter et al., 2004). WT1 is important in the development of many organs but particularly the kidney, where there is also spatial and temporal overlap of BASP1 and WT1 expression. In mouse kidney development, both BASP1 and WT1 are expressed in the forming nephron; in the adult kidney, both are expressed solely in the podocytes lining the glomerulus (Carpenter et al., 2004). BASP1 associates with WT1 in the nucleus. On its own, BASP1 is a weak transcriptional repressor. However, when BASP1 interacts with WT1's N-terminal suppression domain, they together act as a strong transcriptional corepressor of WT1 target genes (Carpenter et al., 2004). For example, in mouse podocyte precursor cells, both WT1 and BASP1 are at the promotors for *Bak*, *C-myc*, and *Podxl* (podocalyxin) (Green et al., 2009). BASP1 is reduced at the podocalyxin promotor during development via sumoylation of BASP1, and this correlates with increased podocalyxin expression. BASP1 is not reduced at the *Bak* and *C-myc* promotors, and consequently, these genes remain downregulated during development (Green et al., 2009). WT1-associated BASP1 is unmyristoylated, which is possibly responsible for its non–cell membrane localization (Carpenter et al., 2004). In the nuclei of podocyte precursor cells, BASP1 is expressed in a speckled pattern, localizing in PML bodies (Green et al., 2009). When BASP1 is sumoylated, it accumulates in the nuclear matrix instead (Green et al., 2009). It has not yet been studied whether chicken BASP1 can be sumoylated. By acting as a transcriptional corepressor with WT1, BASP1 is integral to kidney development.

BASP1 may also have a role in caspase-dependent apoptosis. It is cleaved during apoptosis and present in the cytoplasm of apoptotic HeLa cells, where it moves from the nucleus when HeLa cells are exposed to apoptotic reagents. (Ohsawa et al., 2008). BASP1 is upregulated in human renal tubular epithelial cells under apoptosis-inducing conditions. In these cells, BASP1 is normally found in the perinuclear cytoplasm. During apoptosis, it colocalizes with actin and α-tubulin in the cell periphery (Sanchez-Niño et al., 2010). This peripheral location of actin and tubulin is characteristic of apoptotic cells. In epithelial tissue, cells can form a ring of actin and myosin to push dying cells out of the epithelial layer, thus preventing any gaps in the epithelium (Rosenblatt et al., 2001). As well, microtubules form a cocoon-like structure around the cell during apoptosis

(Sánchez-Alcázar et al., 2007). Overexpression of BASP1 induces apoptotic-like death in tubular cells, and this is prevented by the inhibition of specific caspases. Relatedly, siRNA-mediated knockdown of *BASP1* protects tubular cells from apoptosis (Sanchez-Niño et al., 2010). In tubular cells, BASP1 seems to be specifically involved in albumin-induced apoptosis, as albumin increases both tubular cell apoptosis and BASP1 expression. This increased BASP1 is found mostly in the perinuclear area but also at the cell periphery. Like before, siRNA knockdown of *BASP1* protects tubular cells from albumin-induced apoptosis (Sanchez-Niño et al., 2015).

BASP1 has many diverse modifications and interactions, leading to its presumed roles in cytoskeleton regulation and localization, transcriptional repression, and apoptosis. Any of these functions, solely or in combination, could be the reason for BASP1's presence during development.

BASP1 in neural development

BASP1 is expressed in multiple tissues during development, most prominently in the developing nervous system. Despite its brain-focused name, BASP1 is found in multiple neuronal cell types in both the central and peripheral nervous system (Caroni et al., 1997). Its expression was first described by Widmer and Caroni (1990), using a custom antibody to identify BASP1 on Western blots and on tissue sections. BASP1 is initially widely expressed, before becoming more and more spatially restricted over development to specific organs and then specific cells. In the chicken, at embryonic day 2, BASP1 is expressed in most or all cells; by E3, BASP1 is mostly restricted to the nervous system. It becomes undetectable in the liver at E12 and skeletal muscles at E18. E18 is also the peak of BASP1 expression in the nervous system, declining afterwards. It is still detectable in the nervous system and intestine at birth (Widmer and Caroni, 1990). The distribution of *BASP1* mRNA throughout development, and whether it matches the protein data from Widmer and Caroni (1990), is not yet known. Consequently, neither the accuracy of the custom antibody used to describe protein distribution or whether *BASP1* mRNA is more widely distributed than BASP1 protein is known.

BASP1 expression continues to change postnatally. It is downregulated in motor neurons and at the neuromuscular junction at postnatal week 2 in mice – the timeframe

when muscles stop growing from adding new fibers and of the last phase of synapse elimination. BASP1 is expressed during regeneration at adult mouse intramuscular nerves, and possibly also normally (Caroni et al., 1997; Frey et al., 2000). Elsewhere in the adult nervous system, BASP1 is expressed in the neocortex, in the hippocampal formation, in DRG neurons, in ventral horn neurons, and in terminal Schwann cells at the neuromuscular junction. BASP1 is expressed at very low levels in the thalamus and brain stem, and not expressed at all in the cerebellar cortex. In mature neurons, it is possible that BASP1 is involved in stimulus-induced changes at the synapse, thus creating anatomical plasticity (Frey et al., 2000).

Despite the work implicating BASP1 as a regulator of neurite formation, primarily acting via cytoskeletal regulation, its role during early embryonic neural development is less clear. In terms of cellular location, BASP1 localizes to neurites before preferentially sorting to the axon as labelled by the axonal marker tau. Like GAP43, BASP1 eventually appears in the growth cone, although later. There, BASP1 colocalizes with the presynaptic marker VAMP2, although again later than when VAMP2 first appears. This later appearance could be related to when lipid rafts are increasing in number at the synapse. It is possible that BASP1 is involved in synaptic maturation rather than axon outgrowth (Kashihara et al., 2000). While BASP1 is found in sprouting nerves at the neuromuscular junction, BASP1 is not required for said sprouting (Caroni et al., 1997). Despite having some idea as to BASP1's changing cellular location through development, BASP1's actual function in the developing nervous system has yet to be discovered.

One common way to determine a gene or protein's function is by altering its expression. There have been few knockdown or knockout studies done on *BASP1*. In DRG sensory neuron cultures, *BASP1* knockout causes thin and twisted axons with varicosities. Growth cones also frequently change direction; possibly from a lack of actin resulting in microtubules entering the distal growth cone (Frey et al., 2000). *BASP1* knockout mice have a high mortality. Only 10% survive to adulthood, and when compared to controls, those that survive are hyperactive and weigh less. They have enlarged brain ventricles and almost no stimulus-induced nerve sprouting at the neuromuscular junction (Frey et al., 2000). Axon number in the peripheral nervous

system is normal, but nerve terminals are often oversized, swollen, and surrounded by terminal Schwann cells. These Schwann cells also have hypertrophic processes, which is suggestive of continuous remodeling (Frey et al., 2000). There have been far more studies on BASP1 overexpression; most such studies have focused on later stages of neural development and of the development of the neuromuscular junction. Overexpression of BASP1, GAP43, and MARCKS all change cell morphology (Wiederkehr et al., 1997). Moderate overexpression induces the formation of filopodia, blebs, and long processes, with all 3 proteins being found in said blebs (Wiederkehr et al., 1997). These blebs are very dynamic, appearing and disappearing in 1 to 2 minutes. The blebs contained few cytoskeletal structures and sometimes mitochondria, and there were occasionally filamentous bundles bridging the base of the bleb. GAP43+ blebs colocalized with β-actin and occasionally with phalloidin (Wiederkehr et al., 1997).

BASP1/GAP43/MARCKS overexpression is also associated with a loss of stress fibers, which consist of actin, non-muscle myosin II, and crosslinking proteins (Wiederkehr et al., 1997). When BASP1, GAP43, and MARCKS are highly overexpressed, there is complete collapse of cell structures (Wiederkehr et al., 1997). Endogenously, BASP1 expression is high in E18 rat hippocampal neurons and low in PC12 cells; BASP1 stimulates neurite outgrowth in both (Korshunova et al., 2008). This outgrowth is independent of protein kinase C phosphorylation of BASP1 at Ser6, fibroblast growth factor receptors, Src-family kinases, tau, glycogen synthase kinase 3β, and NCAM. Outgrowth is abrogated by a lack of BASP1 myristoylation (Korshunova et al., 2008). When BASP1 and GAP43 are both overexpressed, neurites are not significantly longer than those from just BASP1 overexpression. While it is possible that BASP1 and GAP43 may be using the same components or pathway, GAP43 outgrowth is NCAM-dependent, unlike BASP1 (Korshunova et al., 2008). In contrast, despite there being a high level of BASP1 expression in the dentate gyrus granule cells, in transgenic mice overexpressing BASP1 there is no difference in nerve sprouting (Caroni et al., 1997). However, in these transgenic mice, postnatal overexpression in motor neurons (starting at P5 to P10) increased nerve sprouting at the neuromuscular junction, both spontaneously and in response to stimuli. There is also an increase in synaptic structure growth (Caroni et al., 1997). Transgenic BASP1 was still present at the neuromuscular

junction at P15, when endogenous expression had stopped (Caroni et al., 1997). Muscles were paralyzed with botulinum toxin A (BTX), which cleaves SNAREs and prevents neurotransmitter vesicle release (Pirazzini et al., 2017). BTX-induced sprouting caused no significant induction of BASP1 expression in control mice. In transgenic mice overexpressing BASP1, BTX-induced sprouting was greatly potentiated, resulting in a greater extent and length of sprouts. As well, changes were seen at doses of BTX too low to induce muscle paralysis (Caroni et al., 1997). α-bungarotoxin is a nicotinic acetylcholine receptor antagonist that also induces muscle paralysis (Young et al., 2003). Paralysis induced by α-bungarotoxin increased synaptic density at the neuromuscular junction in transgenic BASP1 overexpressing mice (Caroni et al., 1997). Increasing BASP1 expression only had an effect to a certain point: sprouting potentiation was similar whether transgenic mice were homozygous or heterozygous for overexpressed BASP1 (Caroni et al., 1997). Transgenic overexpression of GAP43 also caused nerve sprouting, but in a different pattern than BASP1 (Caroni et al., 1997). It is possible that BASP1- and GAP43-induced sprouting may be induced by a decrease in neurotransmitter release, as both increase with dysfunction on either the presynaptic or postsynaptic side. This could be from BASP1 and GAP43 sensing a lack of change in the cell membrane from neurotransmitter exocytosis. Additionally, terminal Schwann cells may also be mediating growth signals induced by reduced neurotransmitter release, as they are known to be involved in sprouting at the neuromuscular junction and respond to such changes. However, there was no difference observed in terminal Schwann cells between the transgenic and control mice (Caroni et al., 1997). While knockout / knockdown and overexpression studies have given some clues as to the function of BASP1 in neural development, these functions still have no clear method of action, and there is still very little on early development.

Rational and hypothesis

Cytoskeletal dynamics are important to early neural development, and BASP1, when expressed in clusters along the cell membrane, seems to be a cytoskeletal regulator. Changes in BASP1 expression affect the actin cytoskeleton, and BASP1 binds to the actin filament regulators PIP_2 and CapZ. However, BASP1 can also, with WT1, influence

development by acting as a transcriptional corepressor. As BASP1 is highly expressed in the developing nervous system, it is possible that BASP1 is involved in regulating changes in the neuronal cytoskeleton or by regulating transcription of pro- or anti-differentiation genes. Current evidence points to the former: BASP1 seems to be involved in neurite / axon outgrowth and neuromuscular junction sprouting. However, BASP1 is not necessary for sprouting, and could possibly be involved in synapse maturation instead. As of now, published studies on BASP1 have been on either cell cultures or on *in vivo* studies occurring much later than BASP1 initially appears in development. There have been none at the earliest stages of embryonic development when BASP1 becomes spatially restricted to the nervous system.

In the chicken, BASP1 localization in the neural tube coincides with the differentiation of neurons. Consequently, I predict that if extra BASP1 is added through *in ovo* electroporation to the early embryo, there will be tissue disorganization of proliferating cells and differentiating neurons and/or overgrowth of neurites and axons. In tandem, I predict that *in ovo* electroporation to knockdown BASP1 should also result in tissue disorganization of proliferating cells and differentiating neurons and/or less neurite and axon outgrowth.

Chapter 2: Materials and Methods

Plasmids

For overexpression, plasmid pCIG (henceforth "150") was used as a control and as a backbone, and plasmid AI58 was used to induce overexpression of *BASP1*. Plasmid 150 contains chicken β-actin and CMV-IE (cytomegalovirus-immediate early) as promoters and cDNA for nuclear-localizing GFP. Plasmid AI58 contains full length chicken *BASP1* DNA cloned into the multicloning site of plasmid 150, upstream of an internal ribosome entry site (IRES) and the *GFP* cDNA. The chicken *BASP1* DNA was obtained previously by the Iulianella lab, through reverse-transcription PCR on an E4.5 chick using primers based on the chicken *BASP1* NCBI reference sequence. The nuclear-localized GFP of both plasmids facilitated the counting of GFP+ cells with various fluorescent markers in immunofluorescence (below). To generate dsRNA for *BASP1* knockdown, plasmids AI52 and AI53, which contain a 800bp fragment of the chicken *BASP1* cDNA cloned into pCR2.1, were used to make forward (sense) and reverse (antisense) copies of *cBASP1* fragment (respectively), using T7 RNA polymerase and an *in vitro* transcription kit (Invitrogen; see below). The same plasmids were also used for sense and antisense riboprobe synthesis for *in situ* hybridization studies. For knockdown experiments, plasmid pMES was used as a control. It encodes cDNA for cytoplasmic-localized GFP, robustly driven by promotors for chicken β-actin and CMV-IE, and generated GFP expression in the soma and axons of developing neurons. All plasmids were grown in *Escherichia coli* and extracted using the Plasmid DNA Purification kit (Qiagen).

In ovo electroporation and sectioning

Chick embryos were electroporated *in ovo* with either 150 (control), AI58 (BASP1 overexpression), pMES (control), or double-stranded *BASP1* RNA with pMES (*BASP1* knockdown). Eggs were obtained from Dalhousie University's Faculty of Agriculture and incubated starting at 21:30. *In ovo* electroporation was performed the morning of the third day, around E2.5 (Hamburger-Hamilton stages 9 to 11). Embryos were visualized using Tyrodes buffer with india ink. The nucleic acid mixture was

injected near the telencephalon. For overexpression, the mixture consisted of 5 mg/mL plasmid in water with 1 µL 0.5% Far Green per 10 µL DNA. For RNA interference, the knockdown mixture consisted of 5 µL of 500 ng/µL dsRNA, 4 µL of 5 µg/µL pMES, and 1 µL 40% FastGreen in water, with the control mixture containing additional pMES in lieu of dsRNA. Electrodes were placed on either side of the embryo parallel to the anteroposterior axis. Embryos were electroporated with 5 pulses of 20 to 25 V of 50 ms duration, with each pulse separated by 1 second. Eggs were taped closed and incubated for a further 48 or 72 hours (E4.5 and 5.5). Non-electroporated eggs were incubated continuously and collected at E3.5, 4.5, and 5.5 (HH stages 19 to 25).

Embryos were fixed in 4% paraformaldehyde in either PBS or phosphate buffer at 4° for at least 3.5 hours, then washed twice in cold PBS for 10 minutes each. They were equilibrated in 15% sucrose in PBS at 4°, then again with 30% sucrose. For freezing, embryos were embedded in OCT compound and immersed in 2-methylbutane cooled with dry ice, then stored at -80°. Embryos were sectioned on a Leica CM1950 cryostat at -20°. Either 12 µm (immunofluorescence) or 20 µm (*in situ* hybridization) transverse sections were collected from the hindbrain and cervical and thoracic neural tube.

In situ hybridization

For riboprobe synthesis, 1 µg of AI52 linearized with SacI, 4 µL 5X transcription buffer, 2 µL 100 mM DTT, 2 µL DIG 10X nucleotide mix, 1 µL RNasin inhibitor, 1.5 µL T7 RNA polymerase, and nuclease-free H_2O to bring it to 20 µL were combined and incubated at 37° for 2 hours. The reaction was stopped with 2 µL of 0.2 M EDTA, then mixed with 50 µL nuclease-free H_2O, 25 µL 10 M ammonium acetate, and 200 µL 100% ethanol, and kept at -80° overnight. The following day, the probe was spun at 21000 x g for 20 minutes at 4°, the supernatant removed, the pellet washed with 50 µL 70% ethanol, and the tube spun at 21000 x g at 4° for 5 minutes. The supernatant was again removed, and the pellet air dried then dissolved in 20 µL nuclease-free H_2O.

Embryos were prepared as above with RNase-free tools and reagents. After sectioning, slides were washed 3 times in DEPC-treated 1X PBS for 10 minutes each. Sections were coated in hybridization buffer, covered, and incubated at 65° for 1 hour. Riboprobe was added to hybridization buffer, denatured at 70° for 10 minutes, then added

to the slides for incubation at 65° overnight. The following day, slides were washed twice with 2X saline sodium citrate (SSC) with 50% formamide for 30 minutes each at 65° then twice with RNase buffer for 5 minutes each. Slides were incubated for 30 minutes at 37° with 1:500 20 µg/mL RNase A in RNase buffer, followed by washes of twice in RNase buffer for 5 minutes each and twice with 2X SSC with 50% formamide for 5 minutes each. Slides were incubated again at 65° for 1 hour in 2X SSC with 50% formamide, then 2 hours in 1X SSC with 50% formamide. Following incubation, slides were washed three times in 1X TBS for 10 minutes each, blocked for 30 minutes with ISH blocking buffer, then kept at 4° overnight in 1:500 anti-DIG in ISH blocking buffer. The next day, slides were washed 3 times with 1X TBS for 10 minutes each then 3 times with alkaline phosphatase buffer for 10 minutes each. In the dark, staining was developed with 1:50 NBT/BCIP stock in alkaline phosphatase buffer for 3 to 6 hours. Developed slides were subject to at least 3 times 10 minutes washes of 1X TBS followed by at least 3 washes of PBT for 10 to 60 minutes each, until background was sufficiently reduced. For long-term storage, slides were post-fixed for 30 minutes in 4% paraformaldehyde before mounting with CC/Mount tissue mounting medium (Sigma-Aldrich).

Immunofluorescence

Slides were permeabilized in 0.05% PBT for 10 minutes, covered in IF blocking buffer for 1 hour, then covered with primary antibody diluted in blocking buffer and kept at 4° overnight. The following day, slides were washed 3 times in 0.05% PBT for 10 minutes each, then covered with secondary antibodies diluted in blocking buffer for 1 hour, then again washed 3 times in 0.05% PBT for 10 minutes. 1:10000 dilution of 3 mg/mL DAPI in PBS was added for 3 minutes then removed with a 5-minute wash of 0.05% PBT. Slides were mounted with Dako Fluorescent Mounting Medium (Dako). For phalloidin staining, slides were permeabilized for 10 minutes in 0.1% PBT, then covered in a 1:140 dilution of stock solution phalloidin-TRITC (CytoSkeleton Inc.) in PBS for 2 hours. The phalloidin fluoresces red (570-594 nm), which allowed for co-localization with GFP-expressing transfected cells. Slides were then washed with 0.05% PBT for 10 minutes, then stained with DAPI, washed again, and mounted as above. Antibodies and phalloidin are listed in **Table 2** and **Table 3**.

Table 2. List of primary antibodies.

Host	Antibody	Dilution	Company	Catalog number
Sheep	Anti-digoxigenin–alkaline phosphatase	1:500	Roche	11093274910
Rabbit	Anti-GFP	1:500	Invitrogen	A-6455
Rabbit	Anti-NEUROM (rabbit 1a, bleed 2)	1:200	N/A	N/A
Rabbit	Anti-PAX6	1:500	Abcam	ab195045
Rabbit	Anti-phosphohistone H3 (Ser10)	1:300	Millipore	06-570
Rabbit	Anti-SOX2	1:200	Millipore	ab5603
Rabbit	Anti-SOX10	1:500	Abcam	ab27655
Mouse	Anti-Tubulin β3 (clone TuJ1)	1:1000	Covance	MMS-435P-250

Table 3. List of secondary antibodies and phalloidin.

Host	Antibody	Fluorescence	Dilution	Company	Catalog number
Donkey	Anti-rabbit	488	1:1500	Invitrogen	A21206
Donkey	Anti-rabbit	568	1:2000	Invitrogen	A10042
Donkey	Anti-mouse	647	1:1500	Invitrogen	A31571
N/A	Acti-Stain 555 phalloidin	555	1:140	Cytoskeleton	PHDH1

RNA interference

Double-stranded RNA synthesis for RNA interference was based on the procedure by Baeriswyl et al., (2008). AI52 and AI53 were linearized with the endonucleases ScaI and SpeI, respectively. For each linearized plasmid, 2 µg was mixed with 0.8 µL 100 mM rNTPs, 0.5 µL RNasin, 2 µL T7 RNA polymerase, 4 µL 5X transcription buffer, 2 µL 100 mM DTT, and nuclease-free H_2O to bring it to 20 µL. The mixture was incubated at 37° for 2 hours, 2 µL of RNase-free DNase I added, then incubated again at 37° for a further hour. 20 µL nuclease-free H_2O was added, then 2 µL 0.2 M EDTA and 22 µL 10 M ammonium acetate. RNA was precipitated at -80° with at least 2.5 volumes of 100% ethanol for at least 1 hour. The RNA was spun at 21000 x g for 30 minutes at 4° and the supernatant was removed. The ssRNA pellet was washed with 70% ethanol, air dried, and dissolved in 20 µL of DEPC-treated PBS. An equal mass of sense ssRNA solution (from AI52) and antisense ssRNA solution (from AI53) were combined, incubated at 95° for 5 minutes, then allowed to slowly cool to room temperature before storing at -80°.

Image analysis and statistics

In situ hybridization images were viewed and captured with a Zeiss Primo Star and Zeiss Axiocam ERc 5s. Immunofluorescent images were viewed and captured with a Zeiss Axio Observer with apotome structural illuminator and Hamamatsu ORCA-Flash4.0 digital CMOS camera.

The number of SOX2+/GFP+ cells in the marginal zone were compared between the overexpression control and experimental conditions, using the TuJ1+ area to identify differentiating post-mitotic neurons accumulating in the marginal zone of the neural tube. The multipoint tool in ImageJ/Fiji was used to count the number of SOX2+ cells in the marginal zone, the number of GFP+ cells in the marginal zone, and the number of cells that were double positive for SOX2 and GFP. The proportion of SOX2+/GFP+ cells was normalized to the total amount of GFP+ cells, and the Mann-Whitney U test used to compare the 2 groups.

For the *BASP1* knockdown experiments, pMES (control) and *BASP1* dsRNA plus pMES (knockdown) were electroporated in chicken neural tubes at E2.5 as above and the

embryos were allowed to develop 2 days (E4.5) or 3 days (E5.5). The length of axons and distance from the base at the soma to the tip of the axon were compared to measure the "twistedness" of axons as a measure of axonal complexity, which is dependent on the dynamic regulation of the actin cytoskeleton. In Fiji, Simple Neurite Tracer (Longair et al., 2011) was used to determine axon length, and the axon base to tip distance was found using the enclosing radius from Sholl Analysis (Ferreira et al., 2014). The difference between axon length and base to tip distance was found and divided by the base to tip difference to obtain a measure for the axonal length. Using this measure, the mean rank of each sample was found and the Mann-Whitney U test used to compare the sum of mean ranks of the control and *BASP1* knockdown groups at E4.5 and at E5.5. $p < 0.05$ was taken as a statistically significant difference.

Chapter 3: Results

In situ hybridization

Chicken BASP1 protein expression throughout the chick neural tube has been previously described by Widmer and Caroni (1990) using immunohistochemistry. BASP1 was found to be distributed roughly equally along the apicobasal axis of the neural tube (Widmer and Caroni, 1990). However, BASP1's exact location in the neural tube was not clear. As no BASP1 antibody was available, in order to more precisely view *BASP1* expression I used *in situ* hybridization (ISH) to characterize *BASP1* mRNA localization during chick embryogenesis. In addition to showing location and intensity of *BASP1* expression, this also created a baseline of comparison for later experimental manipulations of *BASP1*.

ISH was done on chick embryos at E3.5, 4.5, and 5.5 to examine the change in expression over time (**Figure 4**). Sections were taken at the level of the hindbrain and the cervical and thoracic embryonic spinal cord. In agreement with Widmer and Caroni (1990), *BASP1* expression was concentrated in the developing nervous system and expressed far less in the non-neuronal tissue around the neural tube. At E3.5, *BASP1* was seen faintly in the lateral sides of the ventral neural tube (**Figure 4A**). At E4.5, *BASP1* expression was expanded in the ventral half of the neural tube in the area of the growing marginal zone (**Figure 4B**). These ventral areas correspond to the location of newly developed motor neurons, which are the first neurons in the neural tube to differentiate (Ericson et al., 1992; Kicheva et al., 2014). Expression at E5.5 was similar to that at E4.5, with *BASP1* localized to the marginal zone, and with even greater expression in the ventral half (**Figure 4C**). The more widespread expression in the ventral neural tube corresponds with the location of interneurons differentiating (Kicheva et al., 2014). There was also a ventral (high) to dorsal (low) gradient of *BASP1* expression, corresponding to the difference in the timing of neurogenesis along the neural tube (Dessaud et al., 2010). At all timepoints examined, *BASP1* was present in lateral part of the neural tube and not the medial part, indicating that *BASP1* mRNA is not present in the ventricular zone, the location of progenitor cells. In addition to the neural tube, *BASP1* was also seen in parts of the peripheral nervous system. For example, *BASP1* was present in the

vestibulocochlear nerve adjacent to the otic vesicle at E4.5 (**Figure 4D)**. Altogether, these findings indicate that *BASP1* mRNA is expressed in early chick embryogenesis almost exclusively in differentiated neurons. This contrast somewhat with the older protein expression data from immunohistochemistry (Widmer and Caroni, 1990), where BASP1 protein expression appeared throughout the neural tube and did not solely colocalize with differentiated neurons.

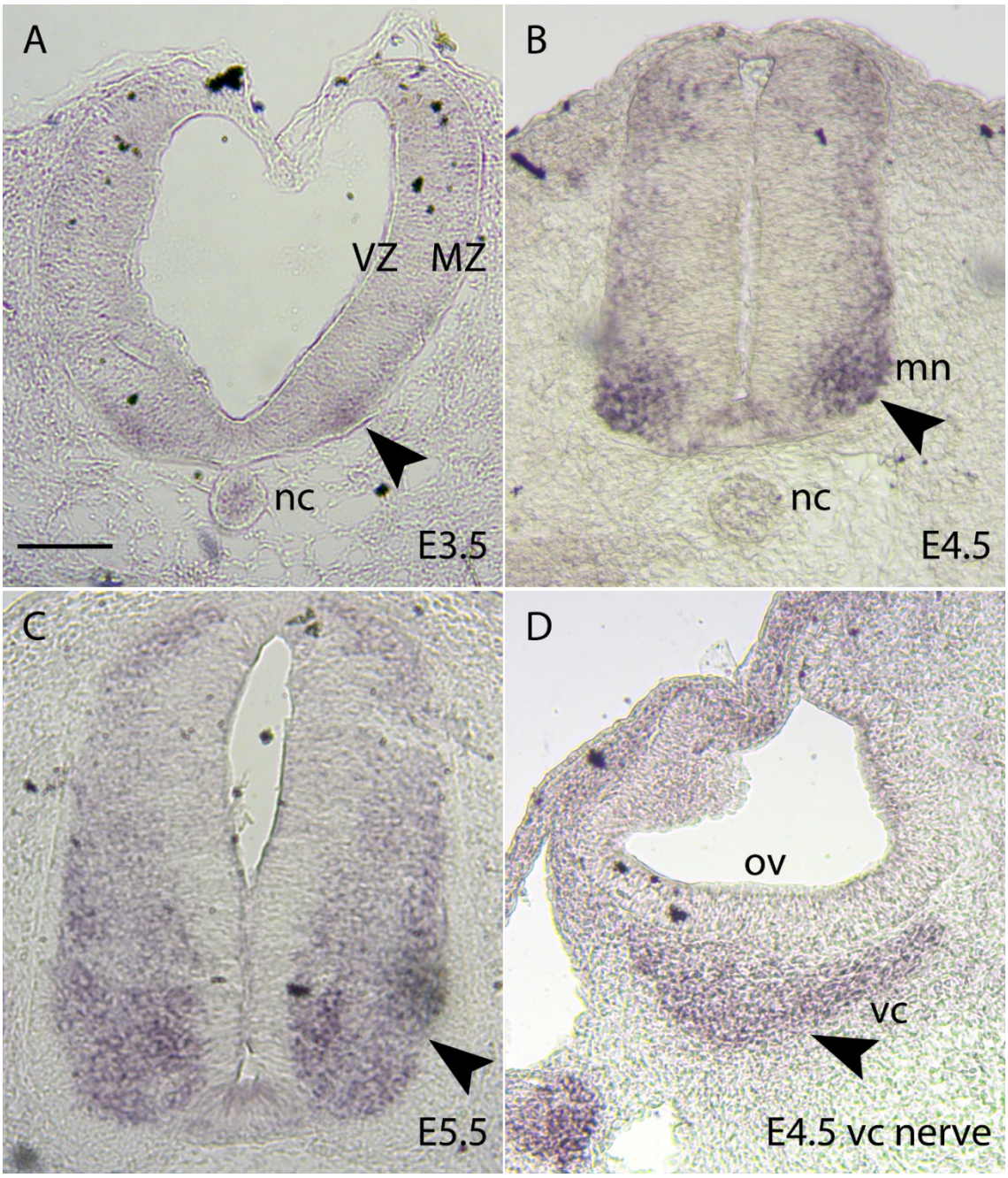

Figure 4. *In situ* hybridization of *BASP1* mRNA (arrowheads) in the developing chick nervous system. *BASP1* mRNA was found in the marginal zone in differentiated neurons. A (E3.5) is from the hindbrain; B (4.5), and C (5.5) are at the level of the cervical and thoracic spinal cord; D (4.5) is from the otic vesicle. Scale bar = 50 µm. VZ = ventricular zone, MZ = marginal zone, nc = notochord, mn = motor neurons, ov = otic vesicle, vc = vestibulocochlear nerve.

As *BASP1* was expressed mainly in differentiated neurons in the early neural tube, it may have a role in early neural development. To assess its potential function, I both increased and decreased BASP1 protein expression in the neural tube using *in ovo* electroporation. To increase expression, the neural tube of E2.5 chick embryos were injected with a bicistronic plasmid containing *GFP* and *BASP1* cDNA. Cells were then transfected with this plasmid using electroporation. This increased the amount of *BASP1* DNA present in a cell, thus increasing the amount of BASP1 protein translated. Control embryos were transfected with a plasmid encoding just *GFP*. Embryos were left to develop for a further 2 days, then collected at E4.5. To decrease protein expression in the neural tube, *BASP1* mRNA was knocked down by electroporating double-stranded *BASP1* RNA in conjunction with a *GFP*-encoding plasmid to visualize transfected neurons. Control embryos were transfected with just the *GFP*-encoding plasmid. Embryos were electroporated at E2.5 and collected at E4.5 and E5.5.

To validate the effect of transfection on *BASP1* mRNA levels, ISH was performed on both control and experimental sections for overexpression and knockdown at E4.5. The sections examined ranged from the rostral hindbrain to the cervical spinal cord. *BASP1* mRNA levels in electroporated controls were compared to that in electroporated experimental conditions. As electroporation occurred unilaterally, *BASP1* expression in the left and right halves of each neural tube section was also compared. In the controls for overexpression (p150, **Figure 5A**) and *BASP1* knockdown (pMES, **Figure 5C**), *BASP1* expression was roughly equal between the left and right halves of the neural tube. For the overexpression experimental condition (AI58), there was a noticeably greater level of *BASP1* mRNA expression in the transfected right half of the neural tube as compared to the untransfected left half or to the control (**Figure 5B**, arrowheads). For the *BASP1* knockdown, the untransfected left side of the experimental condition (dsRNA) had *BASP1* expression roughly equal to that of the control, while the transfected right side had a decrease in *BASP1* expression (**Figure 5D**, arrowheads). To confirm that changes in expression were due to *in ovo* electroporation, a different section of the same embryo for AI58 (not pictured) and for dsRNA (**Figure 5E**) were stained for GFP using immunofluorescence, to visualize transfection. The area of GFP+ cells in **Figure 5E**

corresponded to the area of decreased *BASP1* expression seen in **Figure 5D**. Therefore, *in ovo* electroporation of *BASP1* cDNA and dsRNA were successful in both respectively increasing and decreasing *BASP1* expression in the hindbrain and cervical spinal cord of the developing chick neural tube.

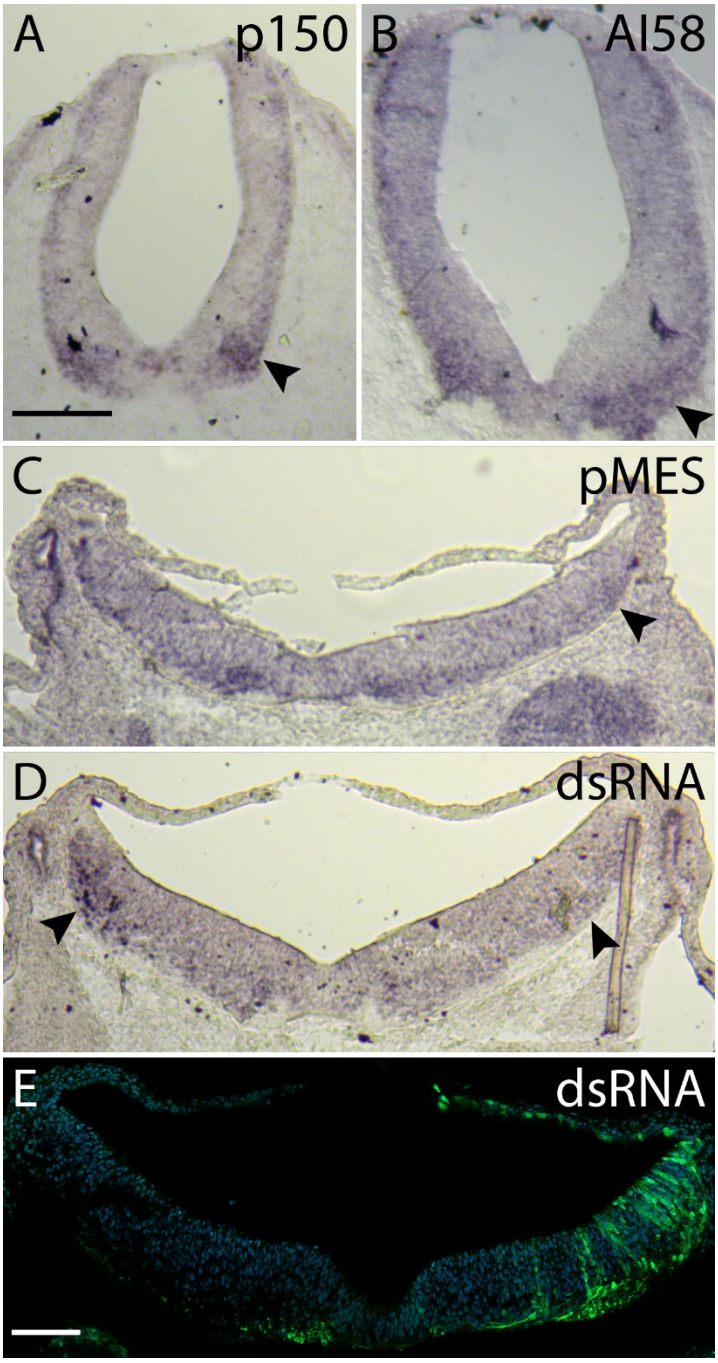

Figure 5. Comparison of *in situ* hybridization of BASP1 (arrowheads) in E4.5 chick neural tubes, between electroporated controls and embryos *in ovo* electroporated for BASP1 overexpression and knockdown. A and B are at the level of the cervical spinal cord; C, D, and E are at the level of the hindbrain. A) Electroporated control for overexpression. B) BASP1 overexpression. C) BASP1 knockdown control with GFP-encoding plasmid. D) BASP1 dsRNA-mediated knockdown, with GFP-encoding plasmid. E) Different section from the same embryo as D) showing GPF expression corresponded to the area of reduced BASP1 expression. Scale bar = 100 μm.

Immunofluorescence

To determine if changes in BASP1 expression affected neural tube development, proteins associated with neural development were examined using immunofluorescence (**Table 4**). Immunofluorescence images were taken at the level of the hindbrain and cervical and thoracic spinal cord.

There is no commercially available antibody for chicken BASP1 and BASP1 antibodies have limited cross-species reactivity (Mosevitsky et al., 1997). As well, the custom-made BASP1 antibodies used by other groups were unavailable. As all electroporated plasmids encoded *GFP*, GFP expression was used instead to identify transfected cells. In the overexpression experimental condition, GFP+ cells were also positive for extra *BASP1* cDNA and thus BASP1 overexpression; in the knockdown experimental condition, GFP+ cells were also positive for *BASP1* dsRNA and thus *BASP1* knockdown.

In many of the immunofluorescence samples TuJ1 was used to denote the marginal zone. TuJ1 is an antibody for class III β-tubulin, which is expressed in neuroblasts and postmitotic neurons but not glia (Caccamo et al., 1989). As there is a high concentration of microtubules in growing axons, class III β-tubulin is highly concentrated in the marginal zone. TuJ1 was also detected in progenitor cell processes along the apicobasal axis. There was no observed difference in TuJ1 staining between the overexpression control and experimental conditions (**Figure 6** through **Figure 10**), nor between the knockdown control and experimental conditions (**Figure 12**, **Figure 13**, and **Figure 15**). Consequently, neither BASP1 overexpression nor knockdown in the early chick neural tube appeared to affect microtubule location or structure.

Table 4. n for each electroporation condition and immunofluorescent stain.

Antibody stain	GFP+ overexpression control (p150)	BASP1 overexpression (AI58)	GFP+ knockdown control (pMES)	BASP1 knockdown (pMES + dsRNA)
NEUROM	5	4	--	--
SOX2	12	10	5	6
SOX10	4	4	--	--
PAX6	6	6	--	--
pHH3	11	11	4	4
Phalloidin (E4.5)	4	5	7	7
Phalloidin (E5.5)	--	--	5	5

BASP1 overexpression

NEUROM (also known as NEUROD4) is a helix-loop-helix transcription factor (Roztocil et al., 1997; UniProt Consortium, 2019b). It is expressed in newly differentiated cells that have stopped proliferating but have not yet moved to the marginal zone. NEUROM+ cells are found at the basal edge of the ventricular zone and throughout the intermediate zone. In the chick spinal cord, NEUROM+ cells appear between E2 and E10 (Roztocil et al., 1997). **Figure 6** shows NEUROM+ cells in the E4.5 neural tube for both control and BASP1 overexpression. NEUROM+ cells were seen in the intermediate zone in both conditions, with no noticeable difference in expression. From this, overexpressed BASP1 did not appear to affect early neuronal differentiation, indicating that BASP1 is likely not critical for early neuron development.

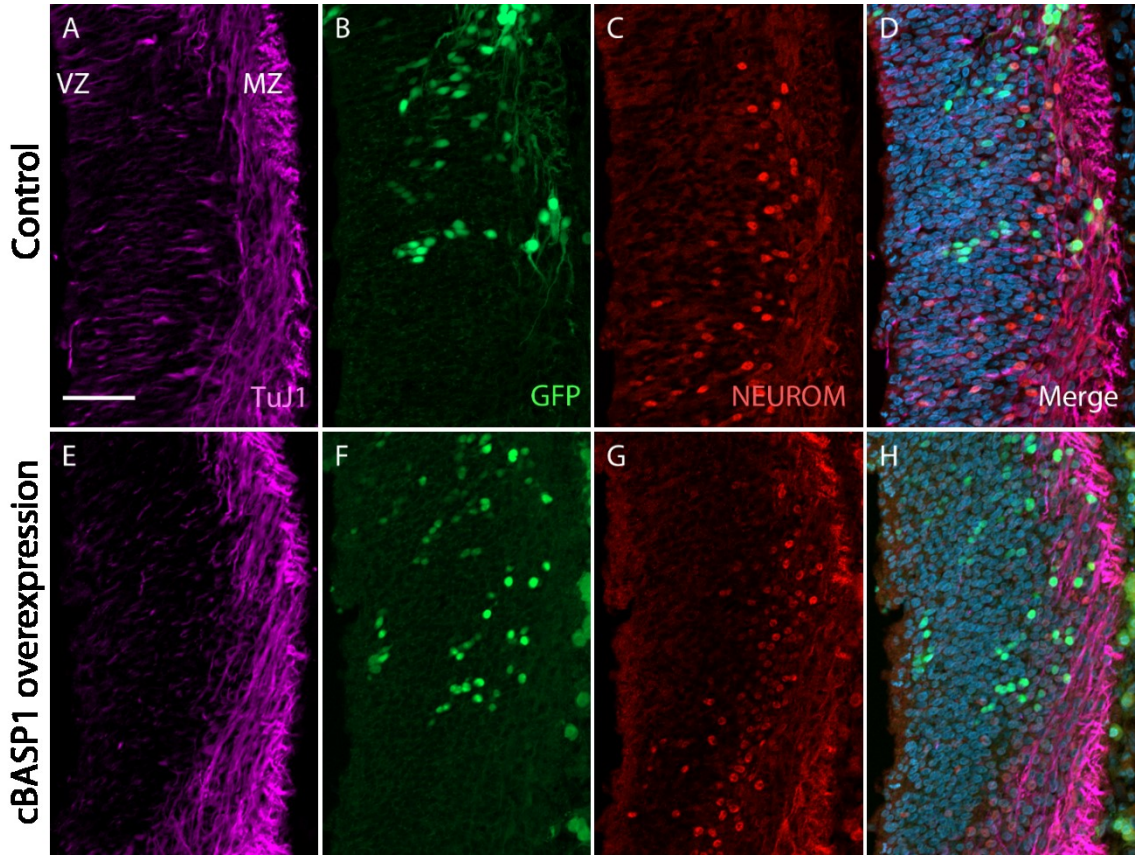

Figure 6. NEUROM expression in the E4.5 chick neural tube with BASP1 overexpression. Embryos were *in ovo* electroporated with a plasmid encoding *GFP* (A through D) or encoding bicistronic *GFP* and *BASP1* cDNA (E through H). Sections from the hindbrain were stained with TuJ1 (A and E), NEUROM (C and G), and DAPI. Transfected cells were GFP+ (B and F). Scale bar = 50 µm. VZ = ventricular zone, MZ = marginal zone.

Another transcription factor expressed in the neural tube is SOX2, which has a variety of functions in early neural development. In neural progenitor cells, SOX2 expression inhibits differentiation; in neural crest cells, SOX2 downregulation induces their migration; in peripheral neurons, SOX2 expression is required for differentiation (Graham et al., 2003; Cimadamore et al., 2011). SOX2+ cells were seen in the ventricular zone in both the control and overexpression conditions (**Figure 7**). However, upon BASP1 overexpression, ectopic SOX2+/GFP+ cells appeared in the intensely TuJ1+ region approximating the marginal zone (**Figure 7F** though **H**, insets). The difference in number of ectopic SOX2+/GFP+ cells between control and overexpression was then measured. For each sample, the number of SOX2+/GFP+ cells in the marginal zone was counted then normalized for total GFP+ cells in the marginal zone, to account for differences in GFP/BASP1 transfection. For the control ($n = 13$, plus one outlier discarded with Grubbs' test at $\alpha = 0.05$), the mean was 0.048 with a standard deviation of 0.044. For the BASP1 overexpression group ($n = 12$), the mean was 0.22 with a standard deviation of 0.11. As the BASP1 overexpression group was not normally distributed (as found using the Shapiro-Wilk test at $\alpha = 0.05$), the non-parametric Mann-Whitney U test was used to compare the control and overexpression groups. The mean ranks of the 2 groups were significantly different ($U = 7$, $p = 0.00012$) at $\alpha = 0.05$. Therefore, there were significantly more SOX2+/GFP+ cells in the marginal zone when BASP1 was overexpressed compared to the control.

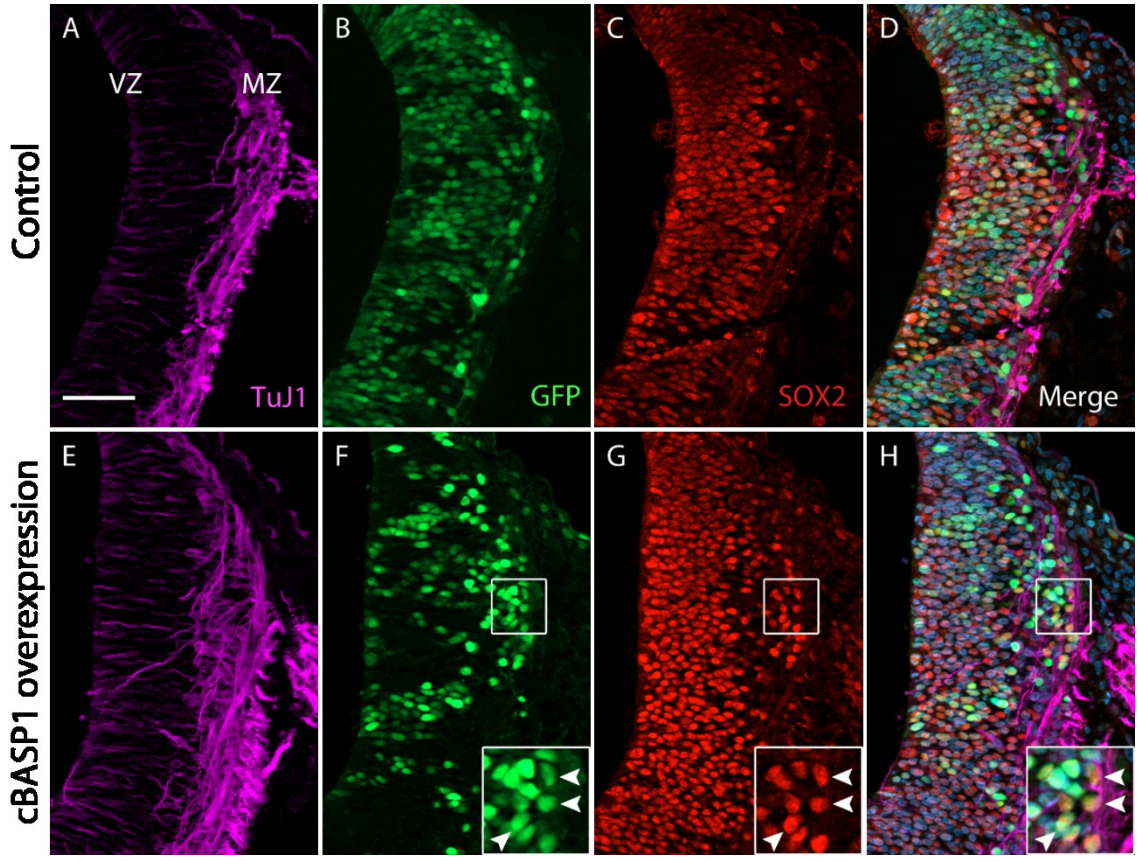

Figure 7. SOX2 expression in the E4.5 chick neural tube with BASP1 overexpression. Embryos were *in ovo* electroporated with a plasmid encoding *GFP* (A through D) or encoding bicistronic *GFP* and *BASP1* cDNA (E through H). Sections from the cervical neural tube were stained with TuJ1 (A and E), SOX2 (C and G), and DAPI. Transfected cells were GFP+ (B and F). While SOX2+ cells can be seen in the ventricular zone for both conditions, for BASP1 overexpression there was also SOX2+/GFP+ cells in the marginal zone (F, G, and H, arrowheads in insets). Scale bar = 50 µm. VZ = ventricular zone, MZ = marginal zone.

As SOX2 is expressed in progenitor cells, it is possible that the ectopic SOX2+/GFP+ cells in the marginal zone in the BASP1 overexpression group are also progenitor cells. However, SOX2 is also expressed in the dorsal root ganglia (Cimadamore et al., 2011), and it is possible that these ectopic SOX2+/GFP+ cells in the marginal zone could have been fate converted to a peripheral neuron phenotype. As SOX10 is transiently expressed in sensory neurons in the DRG (Carney et al., 2006), SOX10 immunostaining was done to see if the ectopic SOX2+/GFP+ cells were positive for this DRG marker. SOX10 expression was unchanged between control and BASP1 overexpression conditions and no SOX10+ cells were seen in the marginal zone (**Figure 8**). Consequently, the ectopic SOX2+/GFP+ cells in embryos overexpressing BASP1 are unlikely to be neural crest cell—derived sensory neurons.

To see if these SOX2+/GFP+ cells in the marginal zone were progenitors, I next looked at a second progenitor cell marker. PAX6 is normally expressed in progenitor cells in the ventricular zone, and slightly later, in the ventral intermediate zone, and not in any peripheral nerve populations (Walther and Gruss, 1991). PAX6+ cells were seen in the ventricular zone in both control and BASP1 overexpression conditions (**Figure 9)**. However, in the overexpression condition, ectopic PAX6+/GFP+ cells were present in the marginal zone, comparable to those seen with SOX2 immunostaining (**Figure 9E** through **H**, insets). Thus, the ectopic cells seen in the marginal zone of BASP1 overexpression embryos are highly likely to be progenitor cells.

Phosphorylated histone H3 (phosphohistone H3 or pHH3) is a marker of mitosis: histone H3 is phosphorylated (predominately at Ser10 in humans) in prophase, metaphase, and telophase (Gurley et al., 1978; Paulson and Taylor, 1982). As only progenitor cells undergo mitosis in the developing neural tube, pHH3 expression was examined to determine if the ectopic SOX2+/GFP+ cells in the marginal zone of BASP1 overexpression samples were mitotically active. In both the control and BASP1 overexpression conditions, pHH3+ cells were only present in the neural tube along the lumen, where progenitor cells normally divide (**Figure 10**). Consequently, while these ectopic SOX2+/GFP+ cells in the marginal zone were positive for 2 different progenitor markers, they did not seem to be mitotically active like other progenitor cells.

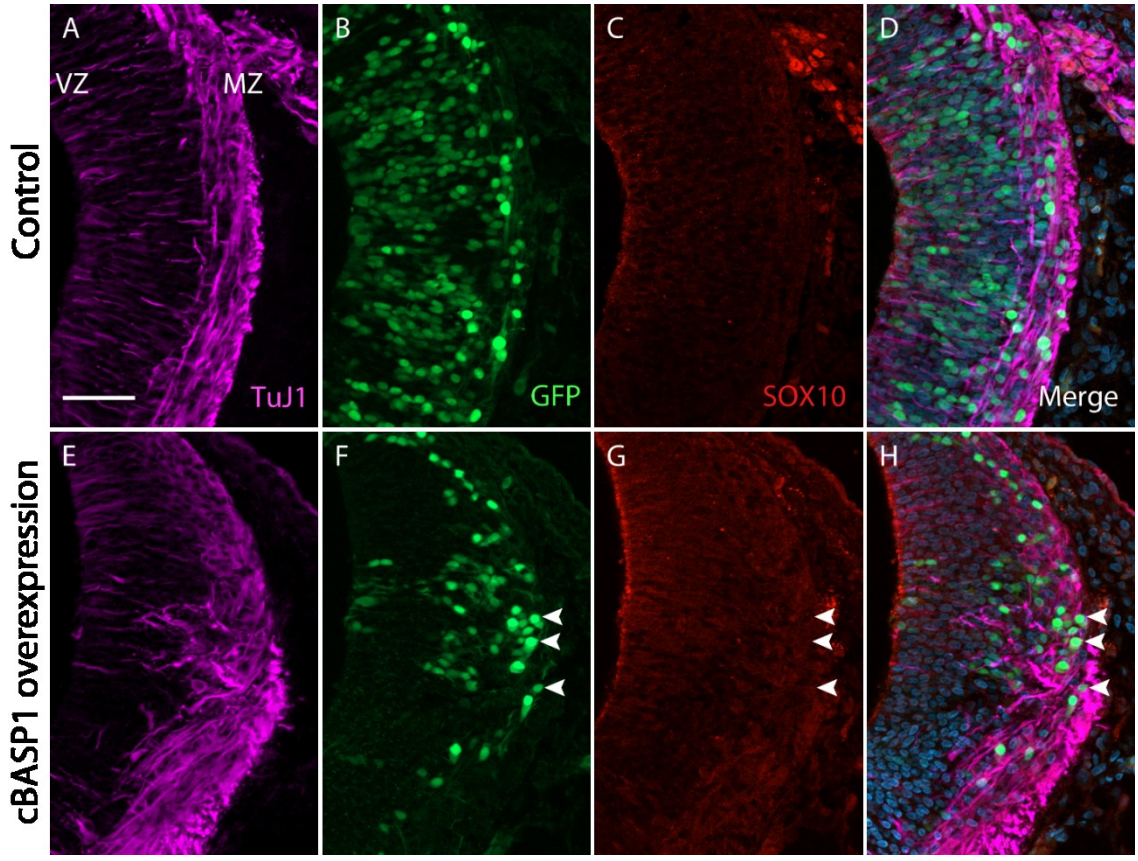

Figure 8. SOX10 expression in the E4.5 chick neural tube with BASP1 overexpression. Embryos were *in ovo* electroporated with a plasmid encoding *GFP* (A through D) or encoding bicistronic *GFP* and *BASP1* cDNA (E through H). Sections from the cervical neural tube were stained with TuJ1 (A and E), SOX10 (C and G), and DAPI. Transfected cells were GFP+ (B and F). SOX10 expression was not seen in the neural tube in either the control (C) or with BASP1 overexpression (G). With BASP1 overexpression, GFP+ cells in the marginal zone were not SOX10+ (F, G, and H, arrowheads). Scale bar = 50 μm. VZ = ventricular zone, MZ = marginal zone.

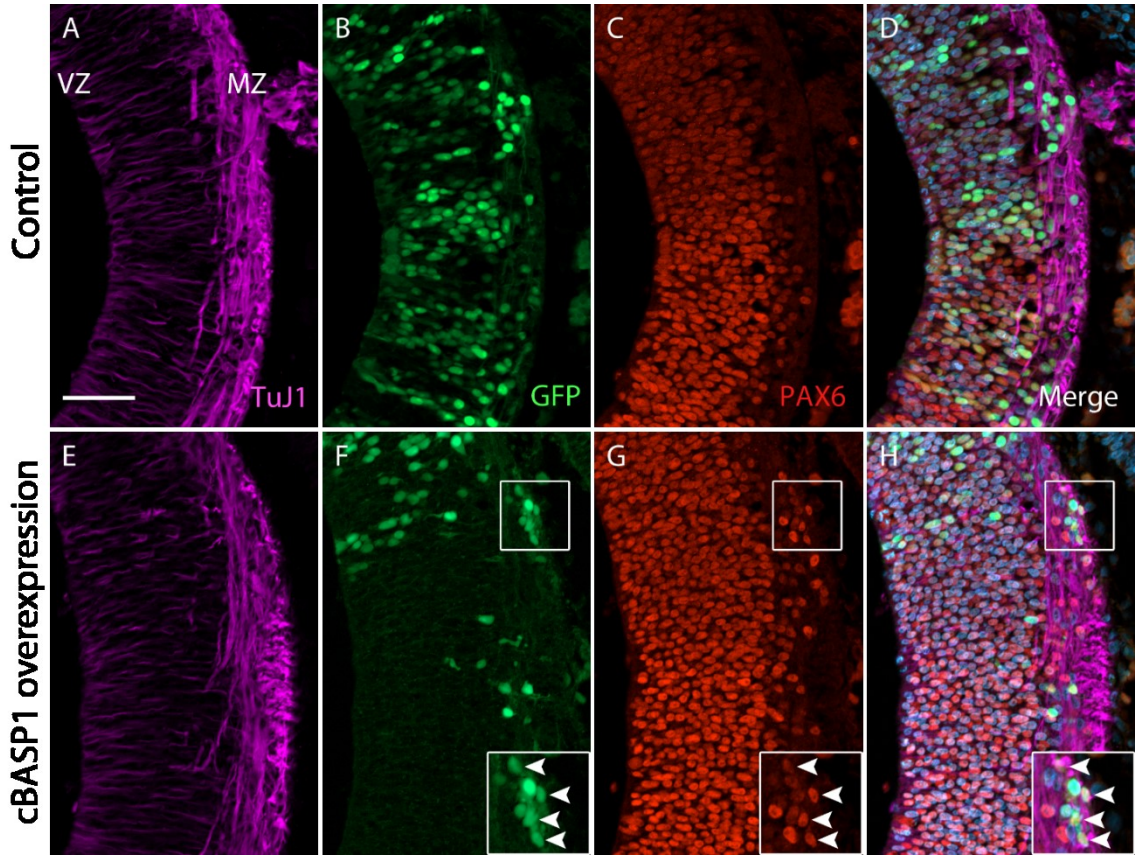

Figure 9. PAX6 expression in the E4.5 chick neural tube with BASP1 overexpression. Embryos were *in ovo* electroporated with a plasmid encoding *GFP* (A through D) or encoding bicistronic *GFP* and *BASP1* cDNA (E through H). Sections from the hindbrain were stained with TuJ1 (A and E), PAX6 (C and G), and DAPI. Transfected cells were GFP+ (B and F). Like with SOX2, there were also ectopic PAX6+/GFP+ cells in the marginal zone with BASP1 overexpression (F, G, and H, arrowheads in insets). Scale bar = 50 µm. VZ = ventricular zone, MZ = marginal zone.

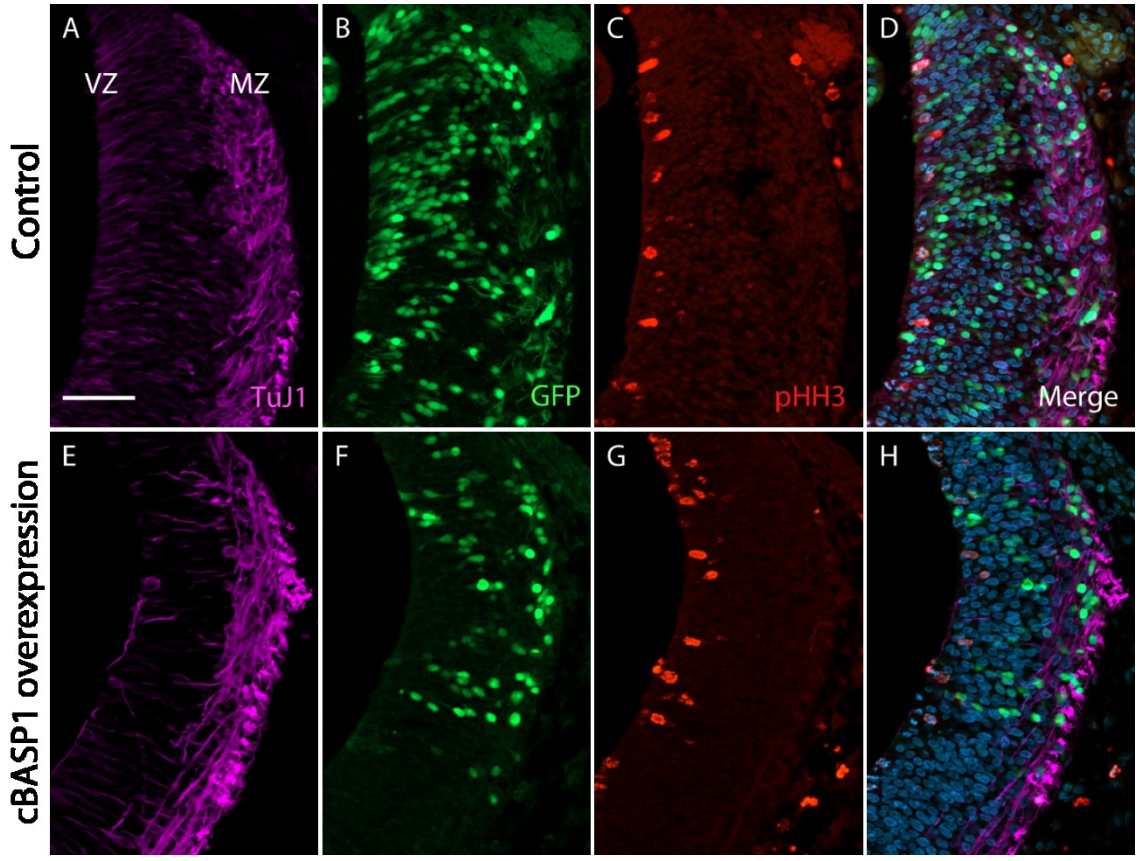

Figure 10. pHH3 expression in the E4.5 chick neural tube with BASP1 overexpression. Embryos were *in ovo* electroporated with a plasmid encoding GFP (A through D) or encoding bicistronic GFP and BASP1 cDNA (E through H). Sections from the hindbrain were stained with TuJ1 (A and E), pHH3 (C and G), and DAPI. Transfected cells were GFP+ (B and F). pHH3+ cells were only seen in the neural tube along the lumen, where progenitor cells normally divide, in both the control (C) and with BASP1 overexpression (G). Scale bar = 50 μm. VZ = ventricular zone, MZ = marginal zone.

Phalloidin is a toxin from the death cap *Amanita phalloides* which binds to actin filaments and prevents actin filament depolymerization *in vivo* (Lengsfeld et al., 1974; Wulf et al., 1979). As BASP1 is involved with actin cytoskeleton localization (Frey et al., 2000; Laux et al., 2000; Odagaki et al., 2009), and actin is involved in neural tube development and axon growth (Spillane et al., 2011; Watanabe et al., 2012; Xu et al., 2013; Das and Storey, 2014; Ganguly et al., 2015; Katsuno et al., 2015), fluorescently-labelled phalloidin staining was used to determine whether BASP1 overexpression affected the actin cytoskeleton in the neural tube. Unexpectedly, there was no discernable difference in phalloidin concentration or location between control and BASP1 overexpression conditions (**Figure 11**). Thus, at least in the developing neural tube, BASP1 overexpression does not seem to disrupt actin expression or structures.

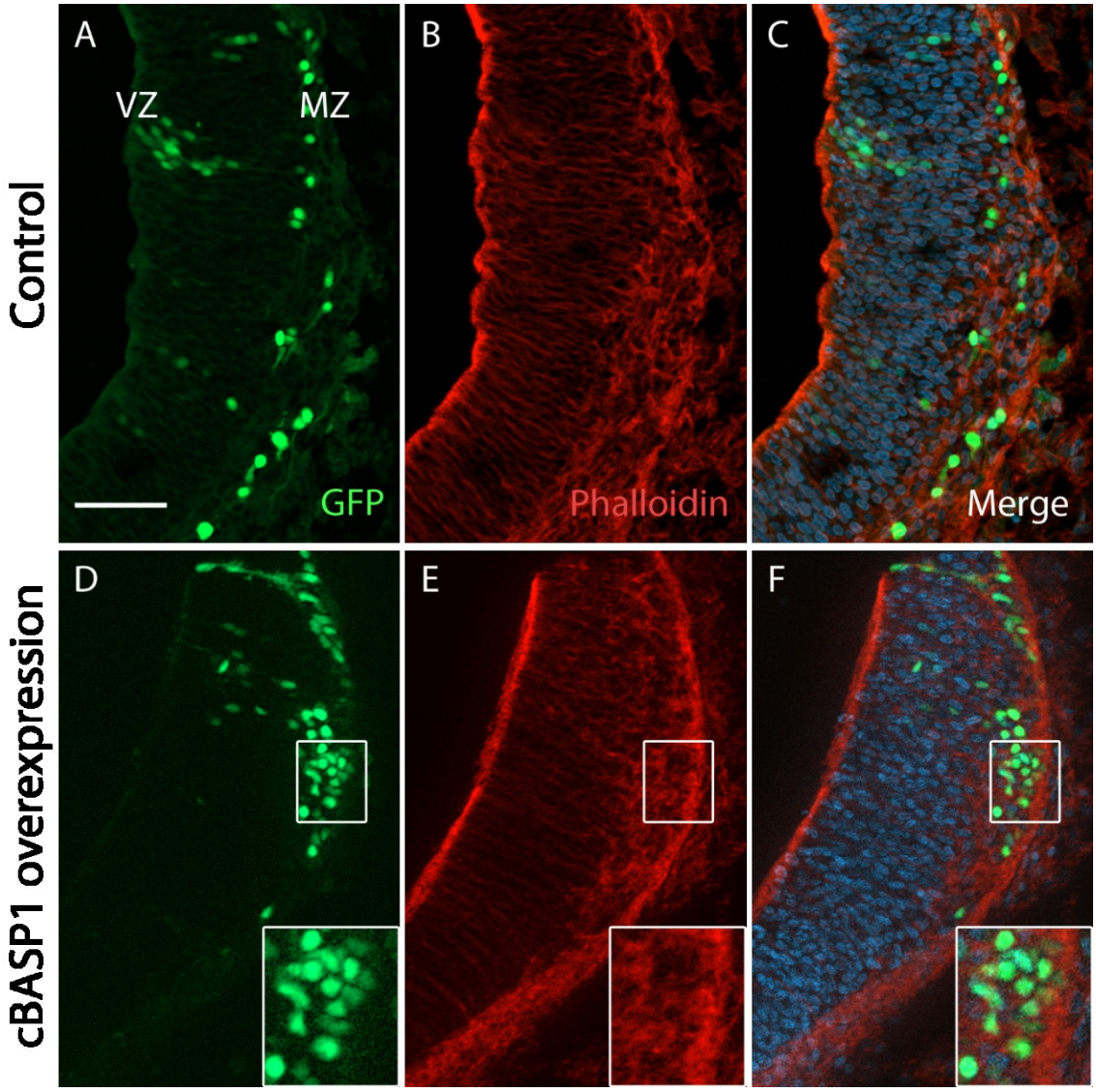

Figure 11. Phalloidin staining in the E4.5 chick neural tube with BASP1 overexpression. Embryos were *in ovo* electroporated with a plasmid encoding *GFP* (A through C) or encoding bicistronic *GFP* and *BASP1* cDNA (D through F). Sections from the hindbrain were stained with phalloidin (B and E) and DAPI. Transfected cells were GFP+ (A and D). No changes in phalloidin intensity or location were observed between the control or with BASP1 overexpression, both overall and around GFP+ cells in the marginal zone (D through F, insets). Scale bar = 50 µm. VZ = ventricular zone, MZ = marginal zone.

BASP1 knockdown

To further study the role of BASP1 in neural development, expression of BASP1 was knocked down using a transcriptional interference approach.. *BASP1* mRNA was knocked down by RNA interference (RNAi), via *in ovo* electroporation of double-stranded chicken *BASP1* mRNA (Pekarik et al., 2003; Stepanek et al., 2005; Baeriswyl et al., 2008). In RNAi, the protein Dicer cuts double-stranded RNA (dsRNA) that is foreign to the cell into small interfering RNAs (siRNA) that are about 21 nucleotides long (Bernstein et al., 2001). One strand of the siRNA is used as a guide by the RNA-induced silencing complex (RISC). RISC cleaves mRNA transcripts that match the siRNA guide, preventing translation of that mRNA (Elbashir et al., 2001). While many siRNA matches are possible for a gene, siRNAs vary in their silencing effectiveness based on their structure. This includes their %GC, stability at the 5' antisense end, and presence of internal repeats or palindromes (Reynolds et al., 2004). Rather than try to find an optimal siRNA, I used an approximately 800 base pair dsRNA transcript of chicken *BASP1*. Using unilateral *in ovo* electroporation of the neural tube, the chicken *BASP1* dsRNA was co-electroporated the plasmid pMES, which encodes a cytoplasmicaly localized GFP. GFP+ cells were assumed to have taken up the *BASP1* dsRNA and be knocked down for *BASP1*, and this was confirmed using ISH (**Figure 5**). *In ovo* electroporation of pMES without dsRNA was used as a control.

As SOX2 expression was abnormal in embryos overexpressing BASP1, its expression was examined in *BASP1* knockdown embryos as well (**Figure 12**). Unlike with overexpression, *BASP1* knockdown did not result in any differences between SOX2 levels or location relative to the control. Thus, decreasing *BASP1* expression does not seem to affect progenitor location in the neural tube.

To determine if *BASP1* knockdown affected mitosis, pHH3 expression was then examined (**Figure 13**). Again, no difference was seen in pHH3 expression or location between the control and *BASP1* knockdown condition. Neither less nor more BASP1 seems to affect mitotic frequency or the location of dividing progenitor cells during neural tube development.

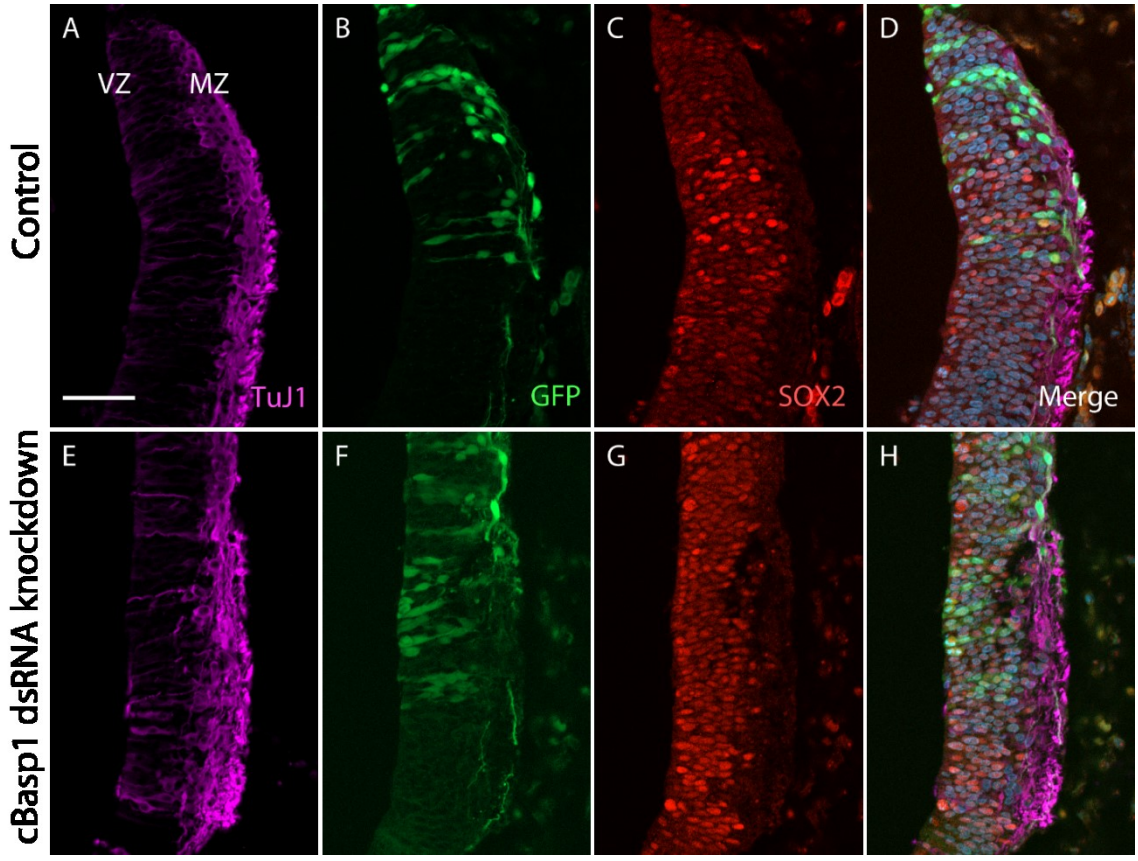

Figure 12. SOX2 expression in the E4.5 chick neural tube with *BASP1* knockdown. Embryos were electroporated with a *GFP*-encoding plasmid solely (A through D) or with *BASP1* dsRNA as well (E through H). Sections from the hindbrain were stained with TuJ1 (A and E), SOX2 (C and G), and DAPI. Transfected cells were GFP+ (B and F). SOX2+ cells were present only in the ventricular zone in both the control (C) and with BASP1 knockdown (G). No ectopic expression of SOX2 was seen with BASP1 knockdown (G, H). Scale bar = 50 µm. VZ = ventricular zone, MZ = marginal zone.

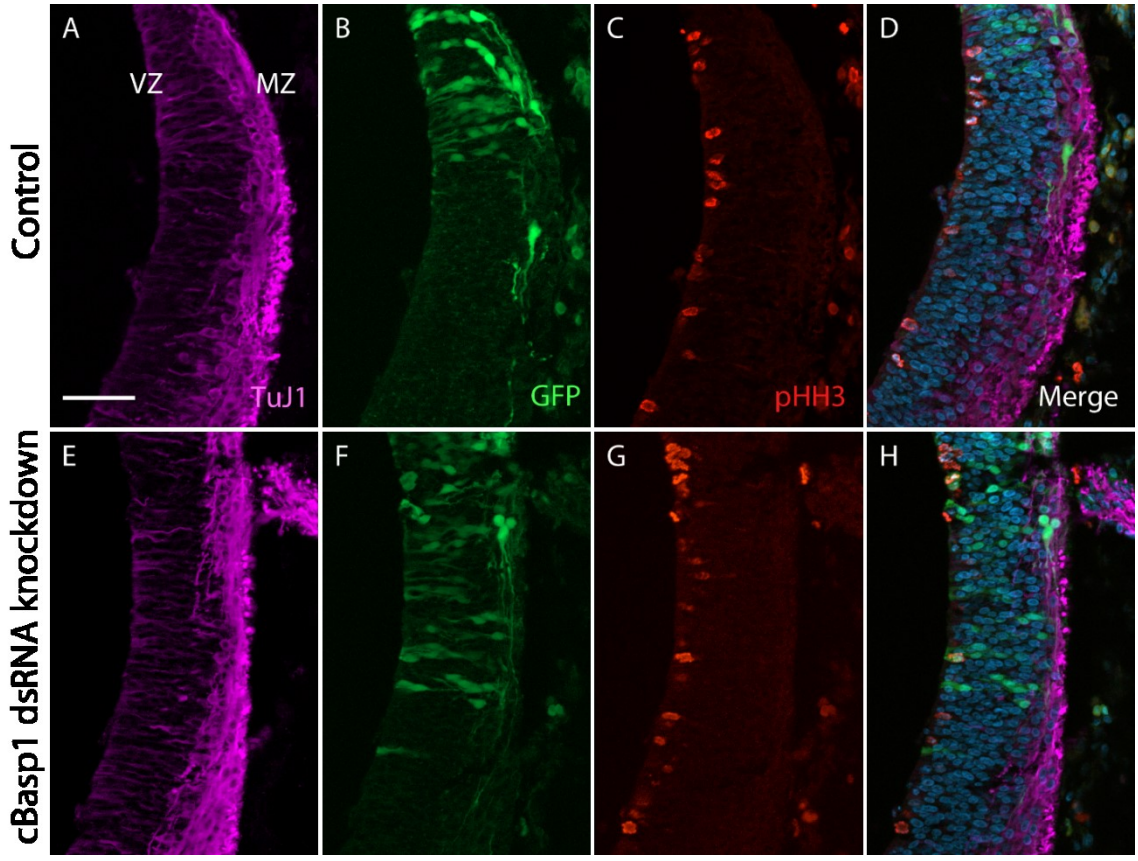

Figure 13. pHH3 expression in the E4.5 chick neural tube with *BASP1* knockdown. Embryos were electroporated with a *GFP*-encoding plasmid solely (A through D) or with *BASP1* dsRNA as well (E through H). Sections from the hindbrain were stained with TuJ1 (A and E), pHH3 (C and G), and DAPI. Transfected cells were GFP+ (B and F). pHH3+ cells were only seen in the neural tube along the lumen, where progenitor cells normally divide, in both the control (C) and with *BASP1* knockdown (G). Scale bar = 50 µm. VZ = ventricular zone, MZ = marginal zone.

While no change in actin expression or location was detected with phalloidin staining with BASP1 overexpression, it is possible that actin could be affected by decreasing BASP1 below a particular threshold. Again using phalloidin staining, there was no discernable change in actin expression or location between the control and *BASP1* knockdown (**Figure 14**). To see if any difference could be found with extra time to produce neurons and grow axons, additional embryos were examined at E5.5, where there was still no visible effect (**Figure 15**). In conclusion, neither BASP1 overexpression nor *BASP1* knockdown in the early chick neural tube appears to affect cytoskeletal dynamics.

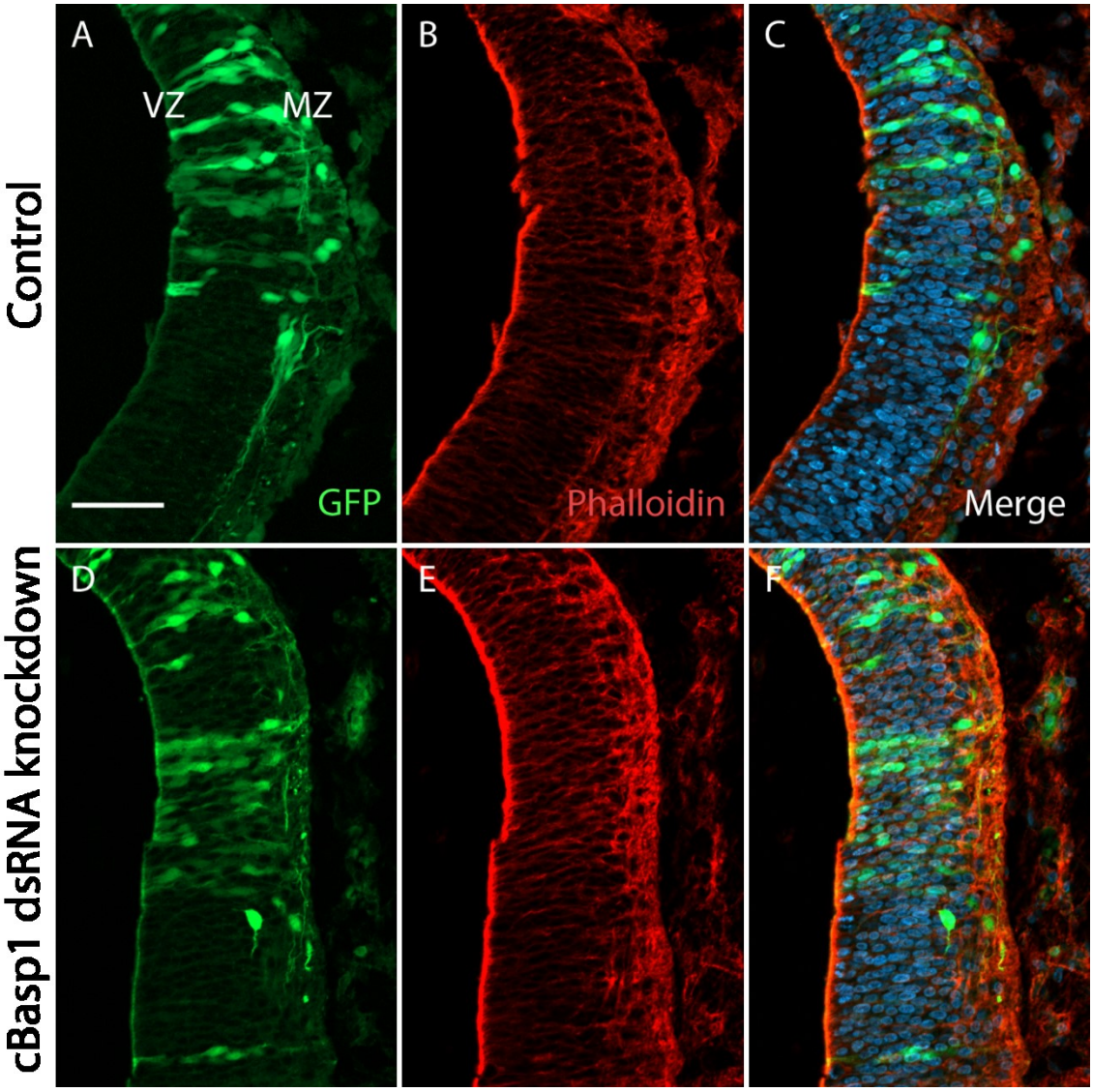

Figure 14. Phalloidin staining in the E4.5 chick neural tube with *BASP1* knockdown. Embryos were electroporated with a *GFP*-encoding plasmid solely (A through C) or with *BASP1* dsRNA as well (D through F). Sections from the hindbrain were stained with phalloidin (B and E), and DAPI. Transfected cells were GFP+ (A and D). No changes in phalloidin intensity or location were observed between the control or with *BASP1* knockdown. Scale bar = 50 μm. VZ = ventricular zone, MZ = marginal zone.

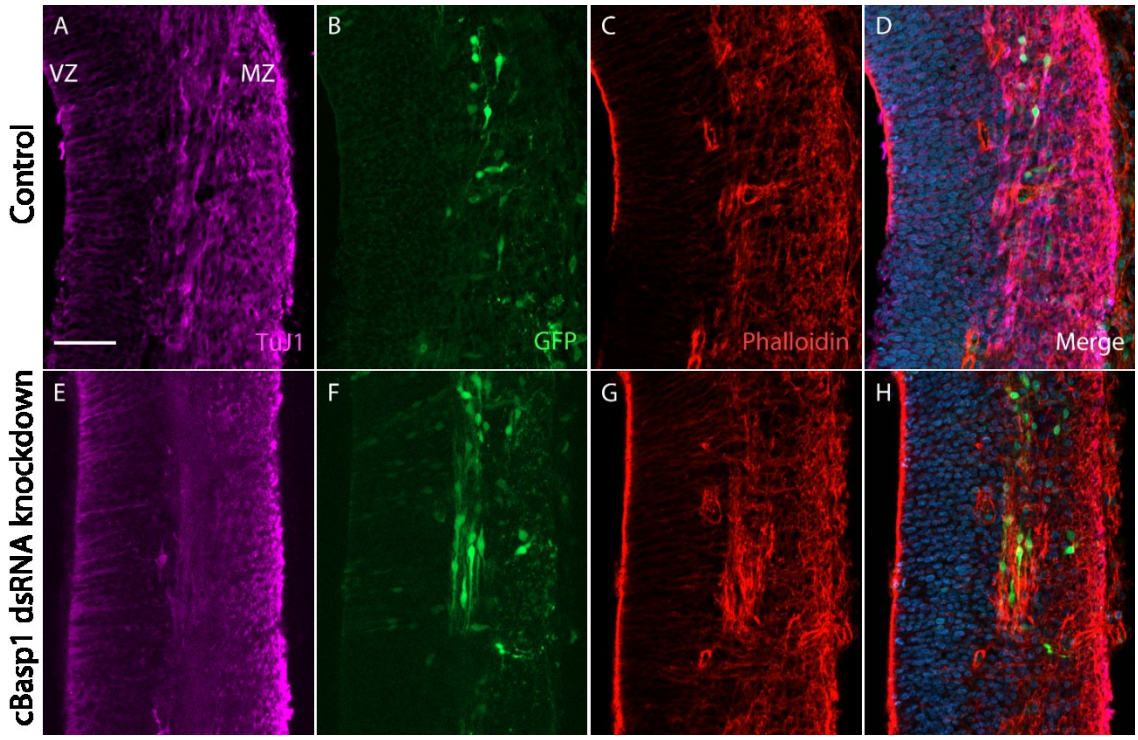

Figure 15. Phalloidin staining in the E5.5 chick neural tube with *BASP1* knockdown. Embryos were electroporated with a *GFP*-encoding plasmid solely (A through D) or with *BASP1* dsRNA as well (E through H). Sections from the hindbrain were stained with TuJ1 (A and E), phalloidin (C and G), and DAPI. Transfected cells were GFP+ (B and F). Both control and *BASP1* knockdown neurons developed normally, with GFP+ cells co-staining with phalloidin and TuJ1. Scale bar = 50 μm. VZ = ventricular zone, MZ = marginal zone.

In Frey et al. (2000), very obvious morphological differences were seen with *BASP1* knockout in cultured DRG neurons: neurites were twisted and frequently changed direction. No such morphology was seen in the axons of *BASP1* knockdown embryos in the chicken neural tube (**Figure 16A** and **B**). However, it is possible that there could be some slight increase in complexities of axonal trajectories, or "twistedness", in *BASP1* knockdown samples. To evaluate this, the twistedness of axons from control and *BASP1* knockdown chick neural tubes were compared at E4.5 (48 hours post-electroporation) and E5.5 (72 hours post-electroporation). The axon length was traced with the Simple Neurite Tracer plugin in ImageJ (Longair et al., 2011) and the straight line distance between the start and end of the trace was found using the final radius measure from the Sholl analysis plugin (Ferreira et al., 2014). The difference between the 2 measurements was found and divided by the final radius measure to account for different axon lengths between samples. As the sample numbers were somewhat small (**Table 5**), a non-normal distribution was assumed, and the Mann-Whitney U test used to compare control and *BASP1* knockdown at E4.5 and E5.5. At E4.5, there was a significant difference in twistedness ($U = 25$, $p = 0.04236$, $\alpha = 0.05$) between control ($n = 9$, mean = 0.169, sd = 0.0691) and *BASP1* knockdown ($n = 12$, mean = 0.113, sd = 0.0285) axons, with the control being more twisted (i.e. complex). However, at E5.5, there was no significant difference ($U = 43$, $p = 0.45326$, $\alpha = 0.05$) between control ($n = 9$, mean = 0.0965, sd = 0.0369) and *BASP1* knockdown ($n = 12$, mean = 0.0871, sd = 0.0392) axon twistedness. Consequently, unlike the results found by Frey et al. (2000) in *in vitro* DRG *BASP1* knockout neurons, *BASP1* knockdown in the chick neural tube *in vivo* did not cause an appreciable increase in the complexity of axon morphology, with in fact a decrease in complexity being seen at E4.5 / 48 hpe (**Figure 16C**). Altogether, these findings support a role for BASP1 in regulating axon morphogenesis, but in a manner opposite to that reported by Frey et al (2000). Namely, my *in vivo* studies suggest that chicken BASP1 knockdown leads to more simple axonal growth trajectories, instead of more complex ones.

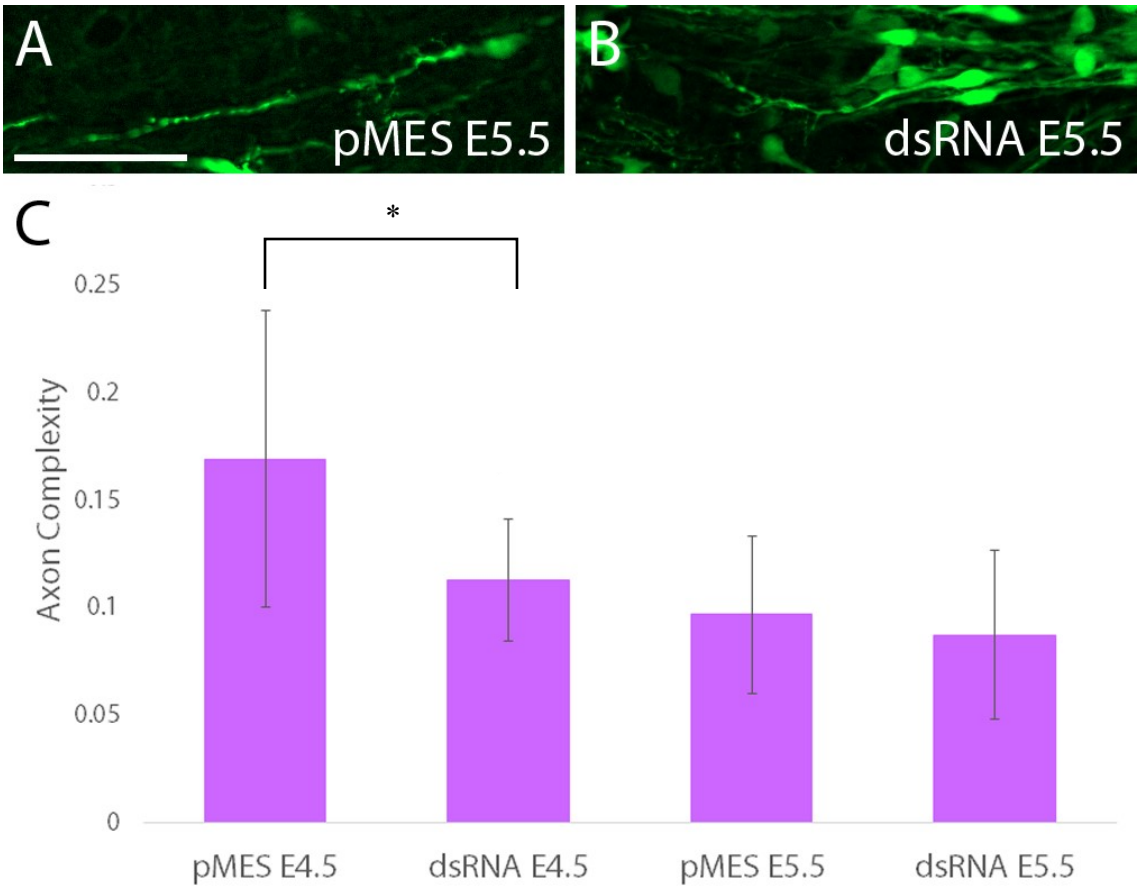

Figure 16. Axon twistedness in both control (pMES) and with *BASP1* knockdown in the chick neural tube at E4.5 and E5.5. A and B) Representative axons from E5.5 chick neural tube of control (A) and *BASP1* knockdown (B). C) Mean axon twistedness of control and *BASP1* knockdown embryos at E4.5 and E5.5. At E4.5, the control axons were significantly more twisted than the *BASP1* knockdown axons; at E5.5 there was no significant difference. Error bars equal the standard deviation. Scale bar = 50 µm.

Table 5. Axon measurements used in measuring axon twistedness between control and *BASP1* knockdown embryos.

Condition + embryonic day	pMES E4.5	dsRNA E4.5	pMES E5.5	dsRNA E5.5
Number of embryos	5	5	4	5
Number of axons	9	12	9	12
Mean axon length (μm)	35.9	48.6	41.2	30.7
Mean distance from axon base to tip (μm)	30.7	43.5	37.3	28.2
(Axon length - distance base to tip)/(distance base to tip)	0.169	0.113	0.096	0.087

Chapter 4: Discussion

Summary of findings

The regulation of the cytoskeleton plays a central role in the formation of the nervous system. This thesis has focused on the role of a regulator of the actin cytoskeleton, BASP1, in the formation of the chicken embryonic hindbrain and spinal cord. The expression profile of *BASP1* was explored and its function in early chick neurogenesis was explored using gain- and loss-of-functions studies. Using *in situ* hybridization (ISH) in the chick neural tube, *BASP1* mRNA was found to colocalize with differentiating neurons, both spatially and temporally. Spatially, *BASP1* was present in the lateral and not medial neural tube; that is, in the marginal zone and not the ventricular zone. Temporally, the location of *BASP1* changed over time coinciding with the timing of various neuron populations differentiating. *BASP1* was also expressed in the developing peripheral ganglia of the embryonic head. ISH also verified that both overexpression of BASP1 and knockdown of *BASP1* did alter the amount of *BASP1* mRNA in the neural tube.

With overexpression of BASP1 protein, there was significantly more ectopic progenitor cells aberrantly in the marginal zone than in the control. These cells were GFP+ (so presumably positive for BASP1 overexpression), and positive for 2 different progenitor cell markers, SOX2 and PAX6. However, as these cells were not pHH3+, they did not seem to be mitotically active. BASP1 overexpression led to no change in NEUROM expression, indicating that BASP1 is not involved in early neuronal differentiation. As well, BASP1 overexpression did not lead to any difference in phalloidin staining, despite previous studies indicating that BASP1 is involved in regulating actin (Frey et al., 2000; Laux et al., 2000; Odagaki et al., 2009).

In contrast to the overexpression studies, the knockdown of *BASP1* in the chick neural tube, did not result in the aberrant formation or positioning of ectopic GFP+/SOX2+ cells in the marginal zone. As with the overexpression, with *BASP1* knockdown there was no change in pHH3 expression at E4.5, and no change in phalloidin staining at E4.5 or E5.5. Unlike the twisted axons in mouse *Basp1* knockout DRG sensory neuron cultures reported in Frey et al. (2000), *BASP1* knockdown axons in the

chick neural tube were not significantly more twisted or complex at E4.5 or E5.5. Indeed, at E4.5, *BASP1* knockdown axons *in vivo* were less complex than control axons, but this difference was not observed at E5.5.

Discrepancy between previous and current *BASP1* neural tube expression data

The expression of *BASP1* mRNA in the chick neural tube visualized by ISH was noticeably different than the expression of BASP1 protein visualized previously by Widmer and Caroni (1990) using immunohistochemistry. In the 1990 Widmer and Caroni paper, BASP1 observed ubiquitously at early stages (E2). By E4 and E6, thoracic and cervical sections showed BASP1 present throughout the entire neural tube. In contrast, with ISH, *BASP1* mRNA was only seen in postmitotic neurons in the marginal zone of the developing neural tube, and not in the ventricular zone, which contains proliferating progenitors. The location of *BASP1* mRNA in the marginal zone also developed over time, correlating with the maturation of differentiating neuron populations. Thus, while the previous immunohistochemistry data showed BASP1 protein expression throughout the whole neural tube, the ISH data showed much more restricted BASP1 mRNA expression only in differentiated neurons.

There are several possible reasons why the BASP1 protein expression found by Widmer and Caroni (1990) does not match the mRNA localization. The first is that expression of mRNA and protein could be under different mechanisms of control. For example, there could be post-transcriptional regulation of gene expression or post-translational regulation of protein expression, which would lead to a difference in amount of mRNA versus protein. However, such a mechanism would lead to a broader pattern of mRNA expression as compared to protein, not a more restricted one. Another possible reason is that BASP1 protein could be secreted, and thus present in a greater area than just the cells transcribing *BASP1* mRNA. As BASP1 can be anchored to the cell membrane when myristoylated, it is possible that BASP1 could be secreted in vesicles from membrane blebbing. Only one study has so far been published indicating that BASP1 can be secreted, in the context of slices of the rat olfactory cortex (Mokrushin and Plekhanov, 2001). There have been no publications as of yet describing BASP1 being

secreted during development. Consequently, in the chick neural tube, it is reasonable to assume that BASP1 mRNA and protein are roughly equal in concentration and location.

Another possible reason for the discrepancy may be due to the lower resolution of the immunostaining images initially described by Widmer and Caroni (1990) compared to the ISH data reported in this thesis. It is also important to note that the Widmer and Caroni (1990) study did not use co-immunohistochemistry, making the localization data difficult to interpret. Specifically, BASP1 expression could not be examined in comparison with expression of markers such as SOX2 or TuJ1 that would more precisely indicate BASP1's exact location. This was likely due to the limitations of the time – the lack of good commercial antibodies and more stable multicolour secondary fluorescent dyes, and the advances in fluorescent microscopy that have developed within the past couple decades.

A fourth possibility for the discrepancy in expression is non-specific antibody binding. Firstly, for the immunohistochemistry, samples were incubated in the primary antibody for 4 hours at room temperature. At room temperature, primary antibody binding is usually for 1 to 2 hours, and a longer incubation can lead to non-specific staining (Abcam, 2019; Sino Biological, 2019). Secondly, the anti-BASP1 antibody created by Widmer and Caroni may not have not been specific to just BASP1. For creation of the antibody, homogenized E16 chick brain was centrifuged and proteins collected from the fourth precipitation, done with 57 to 82% ammonium sulfate. BASP1 was purified from this fraction using 2 subsequent SDS-PAGE separations. Both GAP43 and BASP1 migrate slower than expected from mass in SDS-PAGE; this is possibly owing to myristoylation on BASP1's part (Mosevitsky et al., 1997). The presumed BASP1 band from SDS-PAGE was injected into mice to create hybridoma antibodies. These antibodies were tested against Western blots of chick brain homogenate and of the ammonium sulfate fraction. Thus, antibody specificity relied on the BASP1 band containing no other proteins. As this band was identified by its slower than expected movement, possibly owing to BASP1's myristoylation, it is likely that another acylated protein such as GAP43 or MARCKS could be mixed with BASP1. GAP43 was also examined in the same paper by Widmer and Caroni (1990). While GAP43 was in the same precipitated fraction as BASP1 and did migrate slower than expected with SDS-

PAGE, it formed its own band distinct from that of BASP1. As well, the anti-BASP1 antibody was tested against the GAP43 band. As for MARCKS, it too runs slower than expected based on mass in SDS-PAGE (Albert et al., 1987). MARCKS is present throughout the neural tube at Hamburger-Hamilton stages 14 and 15 (about E2 to 2.5) and 20 (E3 to 3.5) (Zolessi and Arruti, 2001). This matches the diffuse expression of BASP1 in the neural tube seen by Widmer and Caroni (1990). Consequently, it is possible that their immunohistochemistry data for BASP1 expression may also have mistakenly contained additional unspecific binding, possibly to MARCKS.

A fifth possible source of discrepancy may be due to the presence of both BASP1 full length protein and shorter processed protein fragments. As mentioned in the Introduction, BASP1 fragments missing amino acids from their C terminal co-exist *in vivo* with full length BASP1 protein (Zakharov et al., 2003). They appear to be formed after *BASP1* mRNA transcription, and could be formed during or post translation (Kropotova et al., 2013). It is possible that the antibody used by Widmer and Caroni (1990) could bind to epitopes on all BASP1 peptides, while the riboprobe used in ISH could only bind to mRNA for full length BASP1. If BASP1 fragments occur from editing of the mRNA transcript, it is possible that the riboprobe (created from an 800 bp *BASP1* fragment) could not bind to these shorter mRNA fragments. Conversely, if BASP1 fragments occur from premature cessation of protein synthesis or from proteolysis, then the riboprobe would not differentiate between the BASP1 isoforms and not give rise to the different expression patterns. Further ISH experiments with shorter riboprobes could demonstrate whether this is the case.

In conclusion, this thesis has significantly refined the BASP1 spatiotemporal expression profile and reveal that *BASP1* mRNA exclusively labels differentiating neurons in the growing marginal zone and peripheral ganglia of the chicken embryonic head and spinal cord.

Ectopic progenitor cells

When BASP1 was overexpressed in the chicken embryonic neural tube, progenitor cells were detected in the marginal zone, which normally contains only differentiated neurons. How could BASP1 overexpression cause this ectopic placement?

One possibility is BASP1 overexpression disrupted localization of actin filaments within these progenitors. Previous research has indicated that BASP1, in combination with PIP_2, is likely involved in tethering actin filaments to the cell membrane (Laux et al., 2000). As well, BASP1 overexpression can potentiate formation of actin-filled filopodia (Wiederkehr et al., 1997). Thus, overexpressing BASP1 in the neural tube may cause increased actin activity or increased actin at the cell membrane. When progenitors differentiate, an actin contractile ring severs them from their apical domain, allowing the cells to move basally (Das and Storey, 2014). BASP1 overexpression could cause premature contraction of this ring, severing progenitors from the apical surface before differentiation. However, no difference was seen in phalloidin staining between overexpression and control samples, indicating there was no difference in actin expression. It is possible though that any disruption in actin localization could be too small or subtle to see. Immunofluorescence images were taken at 200X magnification. When images were taken at a higher magnification (400X), resolution was too poor. More subtle examination of actin expression could involve time-lapse microscopy of apical abscission in BASP1 overexpression slice cultures, similar to that done by Das and Storey (2014). In conclusion, upon BASP1 overexpression *in vivo* no overt changes change in actin distribution were observed. This is in contrast with the previous literature indicating that BASP1 is involved in regulating actin distribution in the cell.

Another possible reason for these ectopic progenitors comes from a 2009 study by Weimer et al., which looked at *Marcks* knockout mice. With knockout, there were ectopic radial glia progenitors in the cerebral cortex, which led to incorrect positioning of neurons and a disruption in cortical lamination. The ectopic radial glia were found in the intermediate zone and cortical plate and most were positive for the progenitor markers SOX2 and PAX6. Simultaneously, there were less PAX6+ cells in the ventricular zone, presumably as a result of the aberrant progenitor migration. BrdU and pHH3 labeling indicated the ectopic radial glia were still mitotically active, contrasting what was seen with BASP1 overexpression in the chicken embryonic neural tube. MARCKS, like BASP1, can be bound to the cell membrane and colocalize with PIP_2 (Laux et al., 2000). As one function of PIP_2 is recruiting proteins that generate cell polarity (Martin-Belmonte and Mostov, 2007), expression of these proteins were next examined in the *Marcks* -/-

mouse cerebral cortex. Normally, the apical membrane domain of radial glia is enriched in polarity-conferring proteins (Götz and Huttner, 2005; Cappello et al., 2006), and disrupting this polarity can change progenitor identity. For example, β-catenin is normally localized to apical adherens junctions and helps block radial glia from becoming intermediate progenitors (Chae et al., 2004; Wrobel et al., 2007). With *Marcks* knockout, numerous cell polarity proteins were no longer restricted to the apical membrane, with CDC42, NUMB, and β-catenin specifically moving to the basolateral parts of the radial glia. *Marcks* -/- radial glia also had discontinuous cell processes. Later migrating cells were unable to use these processes as a scaffold, leading to greater disruption in cortical lamination. Similar results were seen when only MARCKS's myristoylation domain was mutated, indicating that to function in cortical organization, MARCKS must be myristoylated and thus probably anchored to the cell membrane. In summary, in the mouse cerebral cortex MARCKS seems to be involved in maintaining cell polarity at radial glia apical membranes and without MARCKS, progenitors move away from the ventricular zone. Thus, the ectopic progenitors seen with BASP1 overexpression in the chicken embryonic neural tube may also be the result of disruption in cell polarity. Future research could examine changes in the expression and distribution of cell polarity proteins such as CDC42 resulting from BASP1 overexpression.

Of note is that *increasing* the amount of BASP1 had a similar effect to *decreasing* the amount of MARCKS, indicating that BASP1 may work in opposition to MARCKS with respect to regulating cell polarity. As BASP1 also seems to help recruit proteins to the cell membrane, it may be recruiting antagonists of polarity-forming complexes. As well, the presence of additional BASP1 may cause a decrease in MARCKS at the cell membrane by outcompeting MARCKS for space or binding proteins. For example, there may be a limited amount of PIP_2 or myristic acid available in progenitors and additional BASP1 expression could prevent MARCKS from being able to attach to the cell membrane. This could be tested by overexpressing a version of BASP1 without the initial glycine residue that myristic acid binds to. As well, if *MARCKS* knockdown in the chick via *in ovo* electroporation results in the same effects as knockout in the mouse, then BASP1 expression could be examined after *MARCKS* knockdown (and vice versa) to determine whether the two protein regulate each other.

Another notable difference between the ectopic progenitors from *Marcks* knockout and BASP1 overexpression is that only in the former experiment were mitotic cells detected. With BASP1 overexpression, the ectopic progenitors did not co-stain with pHH3, indicating that they were not mitotically active. Examining the BASP1 overexpression ectopic progenitors for another indicator of mitosis, such as BrdU staining, would help confirm whether they were able to enter the cell cycle but not complete it. It is possible that some aspect of BASP1 overexpression or of timing were making these ectopic progenitor cells transition into non-progenitor cell types, perhaps as a result of a lack of anti-differentiation signals. A more longitudinal study of these cells could help determine if they are remaining progenitors or transitioning to another type of cell.

Ectopic progenitor cells were seen only with BASP1 overexpression and not with *BASP1* knockdown. This could be the result of some other protein compensating for a lack of BASP1. For example, *GAP43* knock-in can compensate for *BASP1* knockout at the neuromuscular junction and at some dorsal root ganglia neurons, if the cells did not already have high GAP43 expression (Frey et al., 2000). If MARCKS is acting in opposition to BASP1 with regards to cell polarity, perhaps it too could act as a check against too little BASP1. A combination of *BASP1* knockdown and *MARCKS* or *GAP43* knockdown could address redundancies between these 3 proteins in the formation and migration of neurons.

BASP1 knockdown axon complexity

There was a disparity in axon complexity between what was seen by Frey et al. (2000) in the *in vitro* mouse *BASP1* knockout neurons versus the *in vivo* chicken *BASP1* knockdown neurons reported in this thesis. In the *BASP1* knockout neuronal cultures, axons were described as “thin and strikingly twisted” and could occasionally be rescued by *GAP43* knock-in (Frey et al., 2000). In comparison, *BASP1* knockdown in the chicken embryonic neural tube resulted in axons being *less* twisted/complex than controls at E4.5 (48 hours post-electroporation), but there was no difference by E5.5 (72 hpe). Why was such a discrepancy seen? It could relate to the degree of *BASP1* knockdown. For example, the *BASP1* knockdown in the chick embryo did not have 100% penetration —

in **Figure 5** through **Figure 15**, not every cell on the electroporated side is GFP+. It could be possible that non-affected cells are rescuing BASP1 expression in their neighbours. While there is some evidence that BASP1 can be secreted (Mokrushin and Plekhanov, 2001), there is of yet no evidence that this occurs during neural tube development. Another difference between cell culture knockout versus the *in vivo* knockdown reported here concerns the timing of targeting *BASP1*. The *BASP1* knockout occurred in all cells from their inception whereas the *BASP1* knockdown was initiated only after E2.5, when neurogenesis and possibly *BASP1* mRNA expression was underway. A final difference is that cell cultures are simpler systems and therefore cannot accurately model the anatomical diversity seen *in vivo*. As also seen by Frey et al. (2000), *GAP43* knock-in did compensate for *BASP1* knockout in some neurons. Perhaps the differentiating chick neural tube has enough endogenous GAP43 (or possibly MARCKS) to counter the effects of *BASP1* knockdown. ISH for *GAP43* could be done on *BASP1* knockdown embryos to see if *GAP43* expression is depleted or increased.

A possible explanation of why axons from *BASP1* knockdown neurons were less twisted/complex than the control at E4.5 may be due to a reduction of actin filaments anchored to the cell membrane, resulting in axons having trouble turning. However, no perturbation in actin was seen from the phalloidin stain. As well, inhibition of actin polymerization normally causes more twisted and complex axons (Frey et al., 2000). As the difference in axon complexity disappeared at E5.5, it is also possible that the earlier difference was a statistical error. There was a small sample size for each condition (at E4.5, n = 9 axons from 5 embryos for the control and n = 12 axons from 5 embryos for the knockdown), and the p-value (0.04236) was somewhat close to α (0.05). It would be advisable to repeat the axon measuring with a larger n to see if the previous results are replicable.

Potential sources of error

With both the overexpression and knockdown conditions, GFP expression was assumed to be an accurate representation of BASP1 expression. However, as GFP is not endogenous to the chicken, BASP1 expression could be under regulatory control in a way that GFP expression is not. Additional or reduced *BASP1* cDNA, RNA, or protein would

likely be subject to any control of expression that affects endogenous BASP1 expression, such as transcription factor binding, RNA silencing, or protein degradation. However, as GFP expression (seen with immunofluorescence) matched changes in *BASP1* expression with overexpression or knockdown (seen with ISH), as seen in **Figure 5D** and **E**, it does seem that GFP expression did match BASP1 expression.

Every pair of control and experimental ISH and immunofluorescent images was selected so that both were at roughly the same axial level. However, owing to the limited number of samples for each condition, the axial level was not always an exact match. Consequently, for some image pairs, the width of the neural tube or the marginal zone differed between the control and experimental conditions. As well, sections were done as close to perpendicular to the neural tube rostrocaudal axis as possible. However, occasionally the sectioning was at an angle, and the left or right half of the neural tube appeared wider. This can be seen in **Figure 5B**: BASP1 overexpression did not correlate with an increase in neural tube width and the appearance of such is a sectioning artifact.

The intensely TuJ1+ area of the neural tube was used as an approximation of the marginal zone. However, SOX2+ cells were seen in the marginal zone for control samples, generally on or near the boundary between the TuJ1+ area and the presumed intermediate zone. Consequently, the TuJ1+ area of the neural tube was not an exact match for the marginal zone. Regardless, there were still more SOX2+/GFP+ cells in the outermost marginal zone with BASP1 overexpression as compared to the control, so BASP1 overexpression did correspond to significantly more ectopic progenitors than the control.

Phalloidin staining was used as a measure of actin expression. However, there can be a difference between actin expression and the binding of phalloidin. Firstly, phalloidin binds specifically to actin filaments (F-actin) and not to G-actin (Wulf et al., 1979). As BASP1 seems to be involved with actin filaments (Laux et al., 2000; Odagaki et al., 2009), this likely did not affect the interpretation of the results. Secondly, tissue fixation can alter the structure of proteins such as actin (Hobro and Smith, 2017). Specifically, during the sample imaging, phalloidin staining was found to only work when embryos had been fixed in fresh 4% paraformaldehyde. However, this equally affected control and experimental condition embryos and thus is not likely to be the source of any significant

difference. Thirdly, the binding of phalloidin to actin can be prevented by other actin-binding proteins such as cofilin (McGough et al., 1997). It is possible that changing the expression of BASP1 could alter the expression of some actin-binding protein that could in turn affect phalloidin staining.

For *BASP1* knockdown experiments, electroporation of just the *GFP*-containing plasmid was used as a control. It would have been more rigorous to use an additional control of electroporated non-*BASP1* dsRNA. In adult mammalian cells, addition of long dsRNA causes global inhibition of all proteins in the cell, leading to cell death (Svoboda, 2004). This is however not the case with oocytes or with embryos (Svoboda et al., 2000; Wianny and Zernicka-Goetz, 2000). In the *BASP1* knockdown embryos, no gross morphological differences were seen that would correlate with increased cell death. Therefore, while just a single control was less rigorous, the non-dsRNA control did appear to be sufficient.

Conclusions and future directions

More is now known about the expression and function of BASP1 in the chick neural tube. BASP1 was found to be expressed in all differentiated neurons in the developing amniote central and peripheral nervous system. Changing BASP1 expression in the neural tube did not affect neural differentiation, mitosis, or actin expression, as seen by expression of NEUROM, pHH3, and phalloidin staining, respectively, but did lead to ectopic positions of neural proteins in the marginal zone. The lack of change in phalloidin staining with BASP1 overexpression and knockdown is surprising, given previous research indicating that BASP1 is involved in regulating actin (Frey et al., 2000; Laux et al., 2000; Odagaki et al., 2009). It is likely that BASP1 has some other role besides actin regulation in the developing neural tube.

Given the data from *Marcks* knockout mice (Weimer et al., 2009), it seems likely that BASP1 overexpression causes a disruption in cell polarity, preventing progenitor cells from staying at the apical side of the neural tube. Like MARCKS, it is possible that myristoylated BASP1, anchored on the cell membrane, colocalizes with PIP_2 and helps it recruit polarity-altering proteins to the cell membrane. As BASP1 was exclusively expressed in differentiated neurons, perhaps BASP1's role there is to eliminate the apical

polarity found in progenitor cells. Further research could examine the expression of different polarity-conferring proteins such as β-catenin, CDC42, and NUMB when BASP1 is overexpressed. Another potential area of research would be to illuminate the relationship between BASP1 and MARCKS in the neural tube with regards to polarity. As well, it is still unknown what eventually happens to these ectopic progenitor cells — do they die? Do they differentiate into neurons?

Another finding in contrast with previous literature was that *BASP1* knockdown axons were not seen to be more twisted or complex, unlike those seen with *BASP1* knockout neurons in culture (Frey et al., 2000). This could be a result of the differences between knockdowns and knockouts, chicken and mice, or the *in vivo* versus *in vitro* study approaches. As well, *BASP1* knockdown axons were found to be less complex than control at E4.5, but not at E5.5, possibly reflecting a sample size issue. It would be useful to repeat that experiment with a greater n to see if that was a significant finding.

In conclusion, this thesis has demonstrated that BASP1 is expressed specifically in differentiated neurons, where it may be involved in the change in cell polarity between neural progenitor cells and mature neurons. As the apicobasal polarity of the neural tube is crucial for neural development, elucidating the potential roles of BASP1 will lead to a better understanding of the anatomical organization and function of the brain and spinal cord.

References

Abcam (2019) Immunocytochemistry and immunofluorescence protocol. Available at: https://www.abcam.com/protocols/immunocytochemistry-immunofluorescence-protocol [Accessed November 11, 2019].

Albert KA, Nairn AC, Greengard P (1987) The 87-kDa protein, a major specific substrate for protein kinase C: purification from bovine brain and characterization. PNAS 84:7046–7050.

Alberts B, Johnson A, Lewis J, Raff M, Roberts K, Walter P (2007) Molecular Biology of the Cell, 5th ed. Garland Science.

Alexandre P, Reugels AM, Barker D, Blanc E, Clarke JDW (2010) Neurons derive from the more apical daughter in asymmetric divisions in the zebrafish neural tube. Nature Neuroscience 13:673–679.

Arnold DB, Gallo G (2014) Structure meets function: actin filaments and myosin motors in the axon. Journal of Neurochemistry 129:213–220.

Baas PW, Deitch JS, Black MM, Banker GA (1988) Polarity orientation of microtubules in hippocampal neurons: uniformity in the axon and nonuniformity in the dendrite. PNAS 85:8335–8339.

Baeriswyl T, Mauti O, Stoeckli ET (2008) Temporal Control of Gene Silencing by in ovo Electroporation. In: RNAi: Design and Application (Barik S, ed), pp 231–244 Methods in Molecular Biology. Totowa, NJ: Humana Press. Available at: https://doi.org/10.1007/978-1-59745-191-8_16 [Accessed March 20, 2019].

Bartolini F, Gundersen GG (2006) Generation of noncentrosomal microtubule arrays. Journal of Cell Science 119:4155–4163.

Bene FD, Wehman AM, Link BA, Baier H (2008) Regulation of Neurogenesis by Interkinetic Nuclear Migration through an Apical-Basal Notch Gradient. Cell 134:1055–1065.

Bernstein E, Caudy AA, Hammond SM, Hannon GJ (2001) Role for a bidentate ribonuclease in the initiation step of RNA interference. Nature 409:363–366.

Black MM, Lasek RJ (1979) Axonal transport of actin: Slow component b is the principal source of actin for the axon. Brain Research 171:401–413.

Bryan J, Wilson L (1971) Are Cytoplasmic Microtubules Heteropolymers? PNAS 68:1762–1766.

Burnette DT, Ji L, Schaefer AW, Medeiros NA, Danuser G, Forscher P (2008) Myosin II Activity Facilitates Microtubule Bundling in the Neuronal Growth Cone Neck. Developmental Cell 15:163–169.

Caccamo DV, Herman MM, Frankfurter A, Katsetos CD, Collins VP, Rubinstein LJ (1989) An immunohistochemical study of neuropeptides and neuronal cytoskeletal proteins in the neuroepithelial component of a spontaneous murine ovarian teratoma. Primitive neuroepithelium displays immunoreactivity for neuropeptides and neuron-associated beta-tubulin isotype. Am J Pathol 135:801–813.

Calderón de Anda F, Pollarolo G, Silva JSD, Camoletto PG, Feiguin F, Dotti CG (2005) Centrosome localization determines neuronal polarity. Nature 436:704–708.

Caldwell JE, Heiss SG, Mermall V, Cooper JA (1989) Effects of CapZ, an actin-capping protein of muscle, on the polymerization of actin. Biochemistry 28:8506–8514.

Cammarata GM, Bearce EA, Lowery LA (2016) Cytoskeletal social networking in the growth cone: How +TIPs mediate microtubule-actin cross-linking to drive axon outgrowth and guidance. Cytoskeleton 73:461–476.

Cappello S, Attardo A, Wu X, Iwasato T, Itohara S, Wilsch-Bräuninger M, Eilken HM, Rieger MA, Schroeder TT, Huttner WB, Brakebusch C, Götz M (2006) The Rho-GTPase cdc42 regulates neural progenitor fate at the apical surface. Nat Neurosci 9:1099–1107.

Carney TJ, Dutton KA, Greenhill E, Delfino-Machín M, Dufourcq P, Blader P, Kelsh RN (2006) A direct role for Sox10 in specification of neural crest-derived sensory neurons. Development 133:4619–4630.

Caroni P, Aigner L, Schneider C (1997) Intrinsic Neuronal Determinants Locally Regulate Extrasynaptic and Synaptic Growth at the Adult Neuromuscular Junction. The Journal of Cell Biology 136:679–692.

Carpenter B, Hill KJ, Charalambous M, Wagner KJ, Lahiri D, James DI, Andersen JS, Schumacher V, Royer-Pokora B, Mann M, Ward A, Roberts SGE (2004) BASP1 Is a Transcriptional Cosuppressor for the Wilms' Tumor Suppressor Protein WT1. Mol Cell Biol 24:537–549.

Chae TH, Kim S, Marz KE, Hanson PI, Walsh CA (2004) The hyh mutation uncovers roles for αSnap in apical protein localization and control of neural cell fate. Nat Genet 36:264–270.

Chen VS, Morrison JP, Southwell MF, Foley JF, Bolon B, Elmore SA (2017) Histology Atlas of the Developing Prenatal and Postnatal Mouse Central Nervous System, with Emphasis on Prenatal Days E7.5 to E18.5. Toxicol Pathol 45:705–744.

Chilton JK (2006) Molecular mechanisms of axon guidance. Developmental Biology 292:13–24.

Cimadamore F, Fishwick K, Giusto E, Gnedeva K, Cattarossi G, Miller A, Pluchino S, Brill LM, Bronner-Fraser M, Terskikh AV (2011) Human ESC-Derived Neural Crest Model Reveals a Key Role for SOX2 in Sensory Neurogenesis. Cell Stem Cell 8:538–551.

Compagnucci C, Piemonte F, Sferra A, Piermarini E, Bertini E (2016) The cytoskeletal arrangements necessary to neurogenesis. Oncotarget 7:19414–19429.

Conde C, Cáceres A (2009) Microtubule assembly, organization and dynamics in axons and dendrites. Nature Reviews Neuroscience 10:319–332.

Czech MP (2000) PIP2 and PIP3: Complex Roles at the Cell Surface. Cell 100:603–606.

Das RM, Storey KG (2014) Apical Abscission Alters Cell Polarity and Dismantles the Primary Cilium During Neurogenesis. Science 343:200–204.

Dessaud E, Ribes V, Balaskas N, Yang LL, Pierani A, Kicheva A, Novitch BG, Briscoe J, Sasai N (2010) Dynamic Assignment and Maintenance of Positional Identity in the Ventral Neural Tube by the Morphogen Sonic Hedgehog. PLOS Biology 8:e1000382.

Drechsel DN, Hyman AA, Cobb MH, Kirschner MW (1992) Modulation of the dynamic instability of tubulin assembly by the microtubule-associated protein tau. MBoC 3:1141–1154.

Elbashir SM, Lendeckel W, Tuschl T (2001) RNA interference is mediated by 21- and 22-nucleotide RNAs. Genes Dev 15:188–200.

Ericson J, Thor S, Edlund T, Jessell TM, Yamada T (1992) Early stages of motor neuron differentiation revealed by expression of homeobox gene Islet-1. Science 256:1555–1560.

Ferreira TA, Blackman AV, Oyrer J, Jayabal S, Chung AJ, Watt AJ, Sjöström PJ, van Meyel DJ (2014) Neuronal morphometry directly from bitmap images. Nature Methods 11:982–984.

Fietz SA, Kelava I, Vogt J, Wilsch-Bräuninger M, Stenzel D, Fish JL, Corbeil D, Riehn A, Distler W, Nitsch R, Huttner WB (2010) OSVZ progenitors of human and ferret neocortex are epithelial-like and expand by integrin signaling. Nature Neuroscience 13:690–699.

Finer JT, Simmons RM, Spudich JA (1994) Single myosin molecule mechanics: piconewton forces and nanometre steps. Nature 368:113–119.

Flynn KC, Pak CW, Shaw AE, Bradke F, Bamburg JR (2009) Growth cone-like waves transport actin and promote axonogenesis and neurite branching. Developmental Neurobiology 69:761–779.

Frade JM, Ovejero-Benito MC (2015) Neuronal cell cycle: the neuron itself and its circumstances. Cell Cycle 14:712–720.

Frey D, Laux T, Xu L, Schneider C, Caroni P (2000) Shared and Unique Roles of Cap23 and Gap43 in Actin Regulation, Neurite Outgrowth, and Anatomical Plasticity. The Journal of Cell Biology 149:1443–1454.

Ganguly A, Tang Y, Wang L, Ladt K, Loi J, Dargent B, Leterrier C, Roy S (2015) A dynamic formin-dependent deep F-actin network in axons. J Cell Biol 210:401–417.

Geraldo S, Gordon-Weeks PR (2009) Cytoskeletal dynamics in growth-cone steering. Journal of Cell Science 122:3595–3604.

Götz M, Huttner WB (2005) The cell biology of neurogenesis. Nat Rev Mol Cell Biol 6:777–788.

Graham V, Khudyakov J, Ellis P, Pevny L (2003) SOX2 Functions to Maintain Neural Progenitor Identity. Neuron 39:749–765.

Green LM, Wagner KJ, Campbell HA, Addison K, Roberts SGE (2009) Dynamic interaction between WT1 and BASP1 in transcriptional regulation during differentiation. Nucleic Acids Res 37:431–440.

Gupton SL, Gertler FB (2007) Filopodia: The Fingers That Do the Walking. Sci STKE 2007:re5–re5.

Gurley LR, D'anna JA, Barham SS, Deaven LL, Tobey RA (1978) Histone Phosphorylation and Chromatin Structure during Mitosis in Chinese Hamster Cells. European Journal of Biochemistry 84:1–15.

Halfter W, Dong S, Yip Y-P, Willem M, Mayer U (2002) A Critical Function of the Pial Basement Membrane in Cortical Histogenesis. J Neurosci 22:6029–6040.

Hanson J, Lowy J (1963) The structure of F-actin and of actin filaments isolated from muscle. Journal of Molecular Biology 6:46-IN5.

Hirokawa N (1998) Kinesin and Dynein Superfamily Proteins and the Mechanism of Organelle Transport. Science 279:519–526.

Hobro AJ, Smith NI (2017) An evaluation of fixation methods: Spatial and compositional cellular changes observed by Raman imaging. Vibrational Spectroscopy 91:31–45.

Howard J, Hyman AA (2003) Dynamics and mechanics of the microtubule plus end. Nature 422:753–758.

Janmey PA (1998) The Cytoskeleton and Cell Signaling: Component Localization and Mechanical Coupling. Physiological Reviews 78:763–781.

Kashihara M, Miyata S, Kumanogoh H, Funatsu N, Matsunaga W, Kiyohara T, Sokawa Y, Maekawa S (2000) Changes in the localization of NAP-22, a calmodulin binding membrane protein, during the development of neuronal polarity. Neuroscience Research 37:315–325.

Katsuno H, Toriyama M, Hosokawa Y, Mizuno K, Ikeda K, Sakumura Y, Inagaki N (2015) Actin Migration Driven by Directional Assembly and Disassembly of Membrane-Anchored Actin Filaments. Cell Reports 12:648–660.

Kaufman MH, Bard JBL (1999) The Anatomical Basis of Mouse Development. Gulf Professional Publishing.

Ketschek A, Gallo G (2010) Nerve Growth Factor Induces Axonal Filopodia through Localized Microdomains of Phosphoinositide 3-Kinase Activity That Drive the Formation of Cytoskeletal Precursors to Filopodia. J Neurosci 30:12185–12197.

Kicheva A, Bollenbach T, Ribeiro A, Valle HP, Lovell-Badge R, Episkopou V, Briscoe J (2014) Coordination of progenitor specification and growth in mouse and chick spinal cord. Science 345:1254927.

Korobova F, Svitkina T (2009) Molecular Architecture of Synaptic Actin Cytoskeleton in Hippocampal Neurons Reveals a Mechanism of Dendritic Spine Morphogenesis. MBoC 21:165–176.

Korshunova I, Caroni P, Kolkova K, Berezin V, Bock E, Walmod PS (2008) Characterization of BASP1-mediated neurite outgrowth. Journal of Neuroscience Research 86:2201–2213.

Kropotova E, Klementiev B, Mosevitsky M (2013) BASP1 and Its N-end Fragments (BNEMFs) Dynamics in Rat Brain During Development. Neurochem Res 38:1278–1284.

Laguesse S, Peyre E, Nguyen L (2015) Progenitor genealogy in the developing cerebral cortex. Cell Tissue Res 359:17–32.

Laux T, Fukami K, Thelen M, Golub T, Frey D, Caroni P (2000) Gap43, Marcks, and Cap23 Modulate Pi(4,5)p2 at Plasmalemmal Rafts, and Regulate Cell Cortex Actin Dynamics through a Common Mechanism. The Journal of Cell Biology 149:1455–1472.

Lengsfeld AM, Löw I, Wieland T, Dancker P, Hasselbach W (1974) Interaction of Phalloidin with Actin. PNAS 71:2803–2807.

Lewis AK, Bridgman PC (1992) Nerve growth cone lamellipodia contain two populations of actin filaments that differ in organization and polarity. The Journal of Cell Biology 119:1219–1243.

Liu SC, Derick LH, Palek J (1987) Visualization of the hexagonal lattice in the erythrocyte membrane skeleton. The Journal of Cell Biology 104:527–536.

Longair MH, Baker DA, Armstrong JD (2011) Simple Neurite Tracer: open source software for reconstruction, visualization and analysis of neuronal processes. Bioinformatics 27:2453–2454.

Louvi A, Grove EA (2011) Cilia in the CNS: The Quiet Organelle Claims Center Stage. Neuron 69:1046–1060.

Maekawa S, Murofushi H, Nakamura S (1994) Inhibitory effect of calmodulin on phosphorylation of NAP-22 with protein kinase C. J Biol Chem 269:19462–19465.

Maekawa S, Sato C, Kitajima K, Funatsu N, Kumanogoh H, Sokawa Y (1999) Cholesterol-dependent Localization of NAP-22 on a Neuronal Membrane Microdomain (Raft). J Biol Chem 274:21369–21374.

Martin-Belmonte F, Mostov K (2007) Phosphoinositides Control Epithelial Development. Cell Cycle 6:1957–1961.

Martínez-Cerdeño V, Noctor SC, Kriegstein AR (2006) The Role of Intermediate Progenitor Cells in the Evolutionary Expansion of the Cerebral Cortex. Cereb Cortex 16:i152–i161.

McGough A, Pope B, Chiu W, Weeds A (1997) Cofilin Changes the Twist of F-Actin: Implications for Actin Filament Dynamics and Cellular Function. J Cell Biol 138:771–781.

Medeiros NA, Burnette DT, Forscher P (2006) Myosin II functions in actin-bundle turnover in neuronal growth cones. Nat Cell Biol 8:216–226.

Michelot A, Drubin DG (2011) Building Distinct Actin Filament Networks in a Common Cytoplasm. Current Biology 21:R560–R569.

Miller KE, Suter DM (2018) An Integrated Cytoskeletal Model of Neurite Outgrowth. Front Cell Neurosci 12 Available at: https://www.frontiersin.org/articles/10.3389/fncel.2018.00447/full [Accessed February 22, 2019].

Miyata T (2008) Development of three-dimensional architecture of the neuroepithelium: Role of pseudostratification and cellular ‘community.’ Development, Growth & Differentiation 50:S105–S112.

Mokrushin AA, Plekhanov AY (2001) Immunological Identification of Endogenous Peptides Secreted by Surviving Slices of Rat Olfactory Cortex. Doklady Biological Sciences 378:227–229.

Mosevitsky MI, Capony JP, Skladchikova GYu, Novitskaya VA, Plekhanov AYu, Zakharov VV (1997) The BASP1 family of myristoylated proteins abundant in axonal termini. Primary structure analysis and physico-chemical properties. Biochimie 79:373–384.

Noctor SC, Martínez-Cerdeño V, Ivic L, Kriegstein AR (2004) Cortical neurons arise in symmetric and asymmetric division zones and migrate through specific phases. Nat Neurosci 7:136–144.

Noctor SC, Martínez-Cerdeño V, Kriegstein AR (2008) Distinct behaviors of neural stem and progenitor cells underlie cortical neurogenesis. Journal of Comparative Neurology 508:28–44.

Odagaki S-I, Kumanogoh H, Nakamura S, Maekawa S (2009) Biochemical interaction of an actin-capping protein, CapZ, with NAP-22. Journal of Neuroscience Research 87:1980–1985.

Ohsawa S, Watanabe T, Katada T, Nishina H, Miura M (2008) Novel antibody to human BASP1 labels apoptotic cells post-caspase activation. Biochemical and Biophysical Research Communications 371:639–643.

Okabe S, Hirokawa N (1991) Actin dynamics in growth cones. J Neurosci 11:1918–1929.

Oshima RG (2007) Intermediate filaments: A historical perspective. Experimental Cell Research 313:1981–1994.

Paridaen JTML, Wilsch-Bräuninger M, Huttner WB (2013) Asymmetric Inheritance of Centrosome-Associated Primary Cilium Membrane Directs Ciliogenesis after Cell Division. Cell 155:333–344.

Paulson JR, Taylor SS (1982) Phosphorylation of histones 1 and 3 and nonhistone high mobility group 14 by an endogenous kinase in HeLa metaphase chromosomes. J Biol Chem 257:6064–6072.

Pekarik V, Bourikas D, Miglino N, Joset P, Preiswerk S, Stoeckli ET (2003) Screening for gene function in chicken embryo using RNAi and electroporation. Nat Biotechnol 21:93–96.

Pike LJ (2003) Lipid rafts bringing order to chaos. J Lipid Res 44:655–667.

Pirazzini M, Rossetto O, Eleopra R, Montecucco C (2017) Botulinum Neurotoxins: Biology, Pharmacology, and Toxicology. Pharmacol Rev 69:200–235.

Pollard TD, Cooper JA (2009) Actin, a Central Player in Cell Shape and Movement. Science 326:1208–1212.

Pruyne D, Evangelista M, Yang C, Bi E, Zigmond S, Bretscher A, Boone C (2002) Role of Formins in Actin Assembly: Nucleation and Barbed-End Association. Science 297:612–615.

Rakic P (2003) Elusive radial glial cells: Historical and evolutionary perspective. Glia 43:19–32.

Reynolds A, Leake D, Boese Q, Scaringe S, Marshall WS, Khvorova A (2004) Rational siRNA design for RNA interference. Nat Biotechnol 22:326–330.

Richter-Landsberg C (2008) The Cytoskeleton in Oligodendrocytes. J Mol Neurosci 35:55–63.

Rosenblatt J, Raff M, Cramer LP (2001) An epithelial cell destined for apoptosis signals its neighbors to extrude it by an actin- and myosin-dependent mechanism. Current Biology 11:1847–1857.

Roy S (2016) Waves, rings, and trails: The scenic landscape of axonal actin. J Cell Biol 212:131–134.

Roztocil T, Matter-Sadzinski L, Alliod C, Ballivet M, Matter JM (1997) NeuroM, a neural helix-loop-helix transcription factor, defines a new transition stage in neurogenesis. Development 124:3263–3272.

Ruthel G, Banker G (1998) Actin-dependent anterograde movement of growth-cone-like structures along growing hippocampal axons: A novel form of axonal transport? Cell Motility 40:160–173.

Saker E, Henry BM, Tomaszewski KA, Loukas M, Iwanaga J, Oskouian RJ, Tubbs RS (2016) The Human Central Canal of the Spinal Cord: A Comprehensive Review of its Anatomy, Embryology, Molecular Development, Variants, and Pathology. Cureus 8 Available at: https://www.ncbi.nlm.nih.gov/pmc/articles/PMC5234862/ [Accessed August 9, 2019].

Sánchez-Alcázar JA, Rodríguez-Hernández Á, Cordero MD, Fernández-Ayala DJM, Brea-Calvo G, Garcia K, Navas P (2007) The apoptotic microtubule network preserves plasma membrane integrity during the execution phase of apoptosis. Apoptosis 12:1195–1208.

Sanchez-Niño MD, Fernandez-Fernandez B, Perez-Gomez MV, Poveda J, Sanz AB, Cannata-Ortiz P, Ruiz-Ortega M, Egido J, Selgas R, Ortiz A (2015) Albumin-induced apoptosis of tubular cells is modulated by BASP1. Cell Death & Disease 6:e1644.

Sanchez-Niño MD, Sanz AB, Lorz C, Gnirke A, Rastaldi MP, Nair V, Egido J, Ruiz-Ortega M, Kretzler M, Ortiz A (2010) BASP1 Promotes Apoptosis in Diabetic Nephropathy. J Am Soc Nephrol 21:610–621.

Sanger JW (1975) Changing patterns of actin localization during cell division. PNAS 72:1913–1916.

Schaefer AW, Kabir N, Forscher P (2002) Filopodia and actin arcs guide the assembly and transport of two populations of microtubules with unique dynamic parameters in neuronal growth cones. The Journal of Cell Biology 158:139–152.

Seeley ES, Nachury MV (2010) The perennial organelle: assembly and disassembly of the primary cilium. J Cell Sci 123:511–518.

Sino Biological (2019) Primary Antibody Incubation for Western Blot. Available at: https://www.sinobiological.com/western-blot-antibody-incubation.html [Accessed November 11, 2019].

Spear PC, Erickson CA (2012) Apical movement during interkinetic nuclear migration is a two-step process. Developmental Biology 370:33–41.

Spillane M, Ketschek A, Jones SL, Korobova F, Marsick B, Lanier L, Svitkina T, Gallo G (2011) The actin nucleating Arp2/3 complex contributes to the formation of axonal filopodia and branches through the regulation of actin patch precursors to filopodia. Developmental Neurobiology 71:747–758.

Stepanek L, Stoker AW, Stoeckli E, Bixby JL (2005) Receptor Tyrosine Phosphatases Guide Vertebrate Motor Axons during Development. J Neurosci 25:3813–3823.

Stossel TP (1989) From signal to pseudopod: How cells control cytoplasmic actin assembly. The Journal of Biological Chemistry 264:18261–18264.

Svoboda P (2004) Long dsRNA and silent genes strike back:RNAi in mouse oocytes and early embryos. CGR 105:422–434.

Svoboda P, Stein P, Hayashi H, Schultz RM (2000) Selective reduction of dormant maternal mRNAs in mouse oocytes by RNA interference. Development 127:4147–4156.

Takasaki A, Hayashi N, Matsubara M, Yamauchi E, Taniguchi H (1999) Identification of the Calmodulin-binding Domain of Neuron-specific Protein Kinase C Substrate Protein CAP-22/NAP-22 DIRECT INVOLVEMENT OF PROTEIN MYRISTOYLATION IN CALMODULIN-TARGET PROTEIN INTERACTION. J Biol Chem 274:11848–11853.

Tsai J-W, Lian W-N, Kemal S, Kriegstein A, Vallee RB (2010) An Unconventional Kinesin and Cytoplasmic Dynein Are Responsible for Interkinetic Nuclear Migration in Neural Stem Cells. Nat Neurosci 13:1463–1471.

UniProt Consortium (2019a) BASP1 - Brain acid soluble protein 1 homolog - Gallus gallus (Chicken) - BASP1 gene & protein (version 102). Available at: https://www.uniprot.org/uniprot/P23614 [Accessed August 14, 2019].

UniProt Consortium (2019b) NEUROD4 - Neurogenic differentiation factor 4 - Gallus gallus (Chicken) - NEUROD4 gene & protein (version 108). Available at: https://www.uniprot.org/uniprot/P79766 [Accessed September 11, 2019].

Wade RH, Hyman AA (1997) Microtubule structure and dynamics. Current Opinion in Cell Biology 9:12–17.

Walther C, Gruss P (1991) Pax-6, a murine paired box gene, is expressed in the developing CNS. Development 113:1435–1449.

Watanabe K, Al-Bassam S, Miyazaki Y, Wandless TJ, Webster P, Arnold DB (2012) Networks of Polarized Actin Filaments in the Axon Initial Segment Provide a Mechanism for Sorting Axonal and Dendritic Proteins. Cell Reports 2:1546–1553.

Weimer JM, Yokota Y, Stanco A, Stumpo DJ, Blackshear PJ, Anton ES (2009) MARCKS modulates radial progenitor placement, proliferation and organization in the developing cerebral cortex. Development 136:2965–2975.

Wells AL, Lin AW, Chen L-Q, Safer D, Cain SM, Hasson T, Carragher BO, Milligan RA, Sweeney HL (1999) Myosin VI is an actin-based motor that moves backwards. Nature 401:505–508.

Wianny F, Zernicka-Goetz M (2000) Specific interference with gene function by double-stranded RNA in early mouse development. Nat Cell Biol 2:70–75.

Widmer F, Caroni P (1990) Identification, localization, and primary structure of CAP-23, a particle-bound cytosolic protein of early development. The Journal of Cell Biology 111:3035–3047.

Wiederkehr A, Staple J, Caroni P (1997) The Motility-Associated Proteins GAP-43, MARCKS, and CAP-23 Share Unique Targeting and Surface Activity-Inducing Properties. Experimental Cell Research 236:103–116.

Willis DE, Niekerk EA van, Sasaki Y, Mesngon M, Merianda TT, Williams GG, Kendall M, Smith DS, Bassell GJ, Twiss JL (2007) Extracellular stimuli specifically regulate localized levels of individual neuronal mRNAs. The Journal of Cell Biology 178:965–980.

Wrobel CN, Mutch CA, Swaminathan S, Taketo MM, Chenn A (2007) Persistent expression of stabilized β-catenin delays maturation of radial glial cells into intermediate progenitors. Developmental Biology 309:285–297.

Wulf E, Deboben A, Bautz FA, Faulstich H, Wieland T (1979) Fluorescent phallotoxin, a tool for the visualization of cellular actin. PNAS 76:4498–4502.

Xu K, Zhong G, Zhuang X (2013) Actin, Spectrin, and Associated Proteins Form a Periodic Cytoskeletal Structure in Axons. Science 339:452–456.

Young HS, Herbette LG, Skita V (2003) α-Bungarotoxin Binding to Acetylcholine Receptor Membranes Studied by Low Angle X-Ray Diffraction. Biophys J 85:943–953.

Zakharov VV, Capony J-P, Derancourt J, Kropolova ES, Novitskaya VA, Bogdanova MN, Mosevitsky MI (2003) Natural N-terminal fragments of brain abundant myristoylated protein BASP1. Biochimica et Biophysica Acta (BBA) - General Subjects 1622:14–19.

Zerbino DR et al. (2018) Ensembl 2018 (release 96). Nucleic Acids Res 46:D754–D761.

Zhong G, He J, Zhou R, Lorenzo D, Babcock HP, Bennett V, Zhuang X (2014) Developmental mechanism of the periodic membrane skeleton in axons Singer RH, ed. eLife 3:e04581.

Zolessi FR, Arruti C (2001) Sustained phosphorylation of MARCKS in differentiating neurogenic regions during chick embryo development. Developmental Brain Research 130:257–267.

Appendix A: Solutions

Alkaline phosphatase buffer
41.5 mL dH_2O
5 mL 1M Tris-HCl at pH 9.5
1 mL 5M NaCl
2.5 mL 1M $MgCl_2$
50 µL Tween 20

IF blocking buffer
3% NDS in 0.05% PBT

ISH blocking buffer
1X TBS
1% serum-free blocking reagent (w/v)
0.1% Tween 20
Adjust pH to 7.5 at 60 to 80°

Hybridization buffer
25 mL deionized formamide
12.5 mL 20X saline sodium citrate
250 µL 100 mg/mL tRNA
5 mL 50% dextran sulfate
1 mL 50X Denhardt's solution
500 µL 10% Tween20

0.05% PBT
0.05% Triton-X100 in 1X PBS

0.1% PBT
0.1% Triton-X100 in 1X PBS

RNase buffer
42.5 mL dH_2O
5 mL 5M NaCl
2.5 mL Tris-HCl at pH 8

1X saline sodium citrate with 50% formamide
22.5 mL DEPC-H_2O
25 mL formamide
2.5 mL 20X SSC stock

2X saline sodium citrate with 50% formamide
20 mL DEPC-H_2O
25 mL formamide
5 mL 20X SSC stock